

High-Order Digital Parametric Equalizer Design[†]

Sophocles J. Orfanidis

Department of Electrical & Computer Engineering
Rutgers University, 94 Brett Road, Piscataway, NJ 08854-8058
Tel: 732-445-5017, e-mail: orfanidi@ece.rutgers.edu

November 15, 2005

Abstract

A family of digital parametric audio equalizers based on high-order Butterworth, Chebyshev, and elliptic analog prototype filters is derived that generalizes the conventional biquadratic designs and provides flatter passbands and sharper bandedges. The equalizer filter coefficients are computable in terms of the center frequency, peak gain, bandwidth, and bandwidth gain. We consider the issues of filter order and bandwidth selection, and discuss frequency-shifted transposed, normalized-lattice, and minimum roundoff-noise state-space realization structures. The design equations apply equally well to lowpass and highpass shelving filters, and to ordinary bandpass and bandstop filters.

0. Introduction

Digital parametric audio equalizers are commonly implemented as biquadratic filters [1-15]. In some circumstances, it might be of interest to use equalizer designs based on high-order filters. Such designs can provide flatter passbands and sharper bandedges at the expense of higher computational cost.

In this paper, we present a family of digital equalizers and shelving filters based on high-order Butterworth, Chebyshev, and elliptic lowpass analog prototypes and derive explicit design equations for the filter coefficients in terms of the desired peak gain, peak or cut frequency, bandwidth, and bandwidth gain. We discuss frequency-shifted transposed, normalized-lattice, and minimum roundoff-noise state-space realization structures, as well as structures that allow the independent control of center frequency, gain, and bandwidth.

High-order equalizers have been considered previously by Moorer [3] who used a conformal mapping method based on elliptic functions to map a first-order lowpass digital shelving filter into a high-order elliptic equalizer, and by Keiler and Zölzer [18] who obtained a fourth-order equalizer based on a second-order analog Butterworth prototype.

Our elliptic designs are essentially equivalent to Moorer's, but we follow a direct approach that closely parallels the conventional analog filter design methods and can be applied equally well to all three filter types, Butterworth, Chebyshev, and elliptic.

[†]Published in *J. Audio Eng. Soc.*, vol.53, pp. 1026-1046, November 2005.

We start by designing a high-order analog lowpass shelving filter that meets the given gain and bandwidth specifications. The analog filter is then transformed into a digital lowpass shelving filter using the bilinear transformation. Finally, the digital shelving filter is transformed into a peaking equalizer centered at the desired peak frequency using a lowpass-to-bandpass z-domain transformation [16,17].

1. General Considerations

The design specifications for the digital equalizer are the quantities $\{G, G_0, G_B, f_0, \Delta f, f_s\}$, that is, the peak or cut gain G , the reference gain G_0 (usually set equal to unity), the bandwidth gain G_B , the peak or cut frequency f_0 in HZ, the bandwidth Δf measured at level G_B , and the sampling rate f_s . These are illustrated in Fig. 1 for the Butterworth case. In the elliptic case, an additional gain, G_s , needs to be specified, as discussed in Section 5. The bandwidth is related to the left and right bandedge frequencies f_1, f_2 by $\Delta f = f_2 - f_1$. It is convenient to work with the normalized digital frequencies in units of radians per sample:

$$\omega_0 = \frac{2\pi f_0}{f_s}, \quad \Delta\omega = \frac{2\pi\Delta f}{f_s}, \quad \omega_1 = \frac{2\pi f_1}{f_s}, \quad \omega_2 = \frac{2\pi f_2}{f_s} \quad (1)$$

The starting point of the design method is an equivalent analog lowpass shelving filter, illustrated in Fig. 1, that has the same gain specifications as the desired equalizer, but with peak frequency centered at $\Omega = 0$ and bandedge frequencies at $\pm\Omega_B$.

The analog filter may be transformed directly to the desired digital equalizer by the bandpass transformation between the s and z planes [16]:

$$s = \frac{1 - 2 \cos \omega_0 z^{-1} + z^{-2}}{1 - z^{-2}} \quad (2)$$

The corresponding frequency mapping between $s = j\Omega$ and $z = e^{j\omega}$ is found from (2) to be:

$$\Omega = \frac{\cos \omega_0 - \cos \omega}{\sin \omega} \quad (3)$$

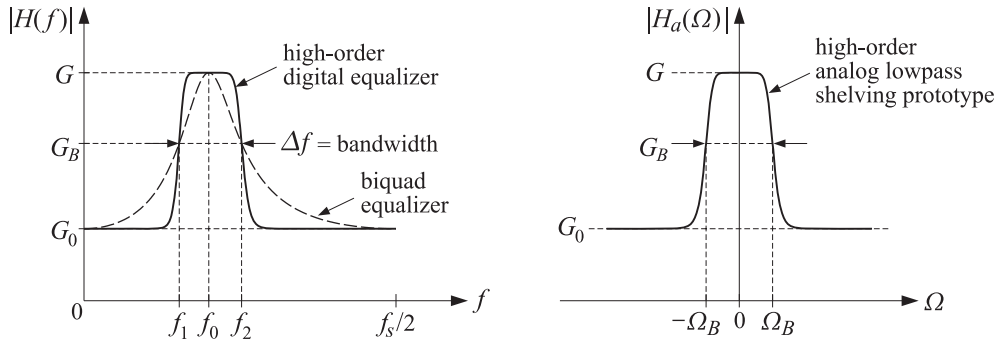


Fig. 1 Specifications of high-order equalizer and the equivalent lowpass analog prototype.

where $\omega = 2\pi f/f_s$ and f is the physical frequency in Hz. The requirement that the bandedge frequencies ω_1, ω_2 map onto $\pm\Omega_B$ gives the conditions:

$$\frac{\cos \omega_0 - \cos \omega_1}{\sin \omega_1} = -\Omega_B, \quad \frac{\cos \omega_0 - \cos \omega_2}{\sin \omega_2} = \Omega_B \quad (4)$$

These may be solved for ω_0 and Ω_B in terms of ω_1 and ω_2 :

$$\Omega_B = \tan\left(\frac{\Delta\omega}{2}\right), \quad \tan^2\left(\frac{\omega_0}{2}\right) = \tan\left(\frac{\omega_1}{2}\right)\tan\left(\frac{\omega_2}{2}\right) \quad (5)$$

where $\Delta\omega = \omega_2 - \omega_1$. Equivalently, we have:

$$\cos \omega_0 = \frac{\sin(\omega_1 + \omega_2)}{\sin \omega_1 + \sin \omega_2} \quad (6)$$

Conversely, Eqs. (4) may be solved for ω_1 and ω_2 in terms of ω_0 and $\Delta\omega$:

$$e^{j\omega_1} = \frac{c_0 + j\sqrt{\Omega_B^2 + s_0^2}}{1 + j\Omega_B}, \quad e^{j\omega_2} = \frac{c_0 + j\sqrt{\Omega_B^2 + s_0^2}}{1 - j\Omega_B} \quad (7)$$

where $\Delta\omega$ enters through $\Omega_B = \tan(\Delta\omega/2)$. Extracting the real parts of Eq. (7), we obtain:

$$\cos \omega_1 = \frac{c_0 + \Omega_B\sqrt{\Omega_B^2 + s_0^2}}{\Omega_B^2 + 1}, \quad \cos \omega_2 = \frac{c_0 - \Omega_B\sqrt{\Omega_B^2 + s_0^2}}{\Omega_B^2 + 1} \quad (8)$$

where we introduced the shorthand notation $c_0 = \cos \omega_0$ and $s_0 = \sin \omega_0$. Eqs. (7) have the proper limits as $\omega_0 \rightarrow 0$ and $\omega_0 \rightarrow \pi$, resulting in the cutoff frequencies (measured at level G_B) of the digital lowpass and highpass shelving equalizers:

$$\begin{aligned} \omega_0 = 0, \quad \omega_1 = 0, \quad \omega_2 = \Delta\omega, \quad & \text{(LP shelf)} \\ \omega_0 = \pi, \quad \omega_1 = \pi - \Delta\omega, \quad \omega_2 = \pi, \quad & \text{(HP shelf)} \end{aligned} \quad (9)$$

The magnitude responses of the high-order analog lowpass shelving Butterworth, Chebyshev, and elliptic prototype filters that we consider in this paper are taken to be:

$$|H_a(\Omega)|^2 = \frac{G^2 + G_0^2 \varepsilon^2 F_N^2(w)}{1 + \varepsilon^2 F_N^2(w)} \quad (10)$$

where N is the analog filter order, ε is a constant, and $F_N(w)$ is a function of the normalized frequency $w = \Omega/\Omega_B$ given by:

$$F_N(w) = \begin{cases} w^N, & \text{Butterworth} \\ C_N(w), & \text{Chebyshev, type-1} \\ 1/C_N(w^{-1}), & \text{Chebyshev, type-2} \\ \text{cd}(NuK_1, k_1), \quad w = \text{cd}(uK, k), & \text{Elliptic} \end{cases} \quad (11)$$

where $C_N(x)$ is the order- N Chebyshev polynomial, that is, $C_N(x) = \cos(N \cos^{-1} x)$, and $\text{cd}(x, k)$ is the Jacobian elliptic function cd with modulus k and real quarter-period K . The parameters k and k_1 are defined in Section 5.

In all four cases, the function $F_N(w)$ is normalized such that $F_N(1) = 1$. The requirement that the bandwidth gain be equal to G_B at the frequencies $\Omega = \pm\Omega_B$ gives a condition from which the constant ε may be determined. Setting $\Omega = \Omega_B$ in Eq. (10), we obtain:

$$|H_a(\Omega_B)|^2 = \frac{G^2 + G_0^2 \varepsilon^2}{1 + \varepsilon^2} = G_B^2 \quad \Leftrightarrow \quad \varepsilon = \sqrt{\frac{G^2 - G_B^2}{G_B^2 - G_0^2}} \quad (12)$$

The analog transfer function $H_a(s)$ corresponding to Eq. (10) is constructed by finding the left-hand s -plane zeros of the numerator and denominator of (10) and pairing them in conjugate pairs. By construction, $H_a(s)$, and hence the equalizer transfer function, will have minimum phase. This is a desirable property because our designs imply that the transfer function of a cut by the same amount as a boost will be the inverse of the corresponding boost transfer function. In terms of its s -plane zeros and poles, $H_a(s)$ may be written in the factored form:

$$H_a(s) = H_0 \left[\frac{1 - s/z_0}{1 - s/p_0} \right]^r \prod_{i=1}^L \left[\frac{(1 - s/z_i)(1 - s/z_i^*)}{(1 - s/p_i)(1 - s/p_i^*)} \right] \quad (13)$$

where L is the number of analog second-order sections, related to the analog filter order by $N = 2L + r$, where $r = 0$, if N is even, and $r = 1$, if N is odd. The notation $[F]^r$ means that the factor F is present if $r = 1$ and absent if $r = 0$. The quantity H_0 is the gain at $\Omega = 0$ (and at the peak frequency $\omega = \omega_0$) and is given in terms of G or G_B as follows:

$$H_0 = \begin{cases} G, & \text{Butterworth and Chebyshev-2} \\ G^r G_B^{1-r}, & \text{Chebyshev-1 and Elliptic} \end{cases} \quad (14)$$

The zeros z_0, z_i and poles p_0, p_i are given in Appendix A.2 for all four filter types. We will use Eq. (13) for the Butterworth, Chebyshev-2, and elliptic designs. For Chebyshev type-1 designs, it is more convenient to use the following form:

$$H_a(s) = H_\infty \left[\frac{z_0 - s}{p_0 - s} \right]^r \prod_{i=1}^L \left[\frac{(z_i - s)(z_i^* - s)}{(p_i - s)(p_i^* - s)} \right] \quad (15)$$

where H_∞ is the gain at $\Omega = \infty$ (and at $\omega = 0$ and $\omega = \pi$) given by:

$$H_\infty = \begin{cases} G_0, & \text{Butterworth and Chebyshev-1} \\ G_0^r G_B^{1-r}, & \text{Chebyshev-2} \\ G_0^r G_s^{1-r}, & \text{Elliptic} \end{cases} \quad (16)$$

The conventional textbook designs [23] of lowpass filters are obtained as special cases of Eqs. (10)–(16) in the limit $G_0 = 0, G = 1$.

For realization purposes, it proves convenient to implement the transformation (2) in two stages by first transforming the analog lowpass shelving filter into a digital lowpass shelving

filter using the ordinary bilinear transformation, and then transforming that into the bandpass peaking equalizer. This two-step process is expressed by writing Eq. (2) in the form [16,17]:

$$s = \frac{1 - \hat{z}^{-1}}{1 + \hat{z}^{-1}} = \frac{1 - 2c_0 z^{-1} + z^{-2}}{1 - z^{-2}} \Leftrightarrow \hat{z}^{-1} = \frac{z^{-1}(c_0 - z^{-1})}{1 - c_0 z^{-1}} \quad (17)$$

Such transformations have been used in the design of the biquadratic equalizer [8] and bandpass and bandstop filters with variable characteristics [19-21].

Under the lowpass transformation from s to \hat{z} , the factored form of Eq. (13) results in a digital lowpass shelving filter of order N that is a cascade of first- and second-order sections in the variable \hat{z} . Then, the lowpass-to-bandpass transformation from \hat{z} to z will yield the bandpass equalizer, centered at ω_0 , as a cascade of second- and fourth-order sections in the variable z , with a net filter order of $2N$.

Thus, the designed equalizer transfer function can be expressed in terms of the variable s , or the variable \hat{z} , or the variable z , in the following equivalent cascaded forms:

$$H(z) = \left[\frac{B_{00} + B_{01}s}{A_{00} + A_{01}s} \right]^r \prod_{i=1}^L \left[\frac{B_{i0} + B_{i1}s + B_{i2}s^2}{A_{i0} + A_{i1}s + A_{i2}s^2} \right] \quad (18a)$$

$$= \left[\frac{\hat{b}_{00} + \hat{b}_{01}\hat{z}^{-1}}{1 + \hat{a}_{01}\hat{z}^{-1}} \right]^r \prod_{i=1}^L \left[\frac{\hat{b}_{i0} + \hat{b}_{i1}\hat{z}^{-1} + \hat{b}_{i2}\hat{z}^{-2}}{1 + \hat{a}_{i1}\hat{z}^{-1} + \hat{a}_{i2}\hat{z}^{-2}} \right] \quad (18b)$$

$$= \left[\frac{b_{00} + b_{01}z^{-1} + b_{02}z^{-2}}{1 + a_{01}z^{-1} + a_{02}z^{-2}} \right]^r \prod_{i=1}^L \left[\frac{b_{i0} + b_{i1}z^{-1} + b_{i2}z^{-2} + b_{i3}z^{-3} + b_{i4}z^{-4}}{1 + a_{i1}z^{-1} + a_{i2}z^{-2} + a_{i3}z^{-3} + a_{i4}z^{-4}} \right] \quad (18c)$$

When $N = 1$, the r -factor is identical to the conventional biquad equalizer [1-15]. For the special cases of lowpass and highpass digital shelving filters, we have $c_0 = \pm 1$, and Eq. (17) reduces to $\hat{z}^{-1} = \pm z^{-1}$. These cases are described only by Eqs. (18a) and (18b).

The algebraic relations among the coefficients of Eq. (18) are straightforward and given in Appendix A.1. In the following sections, we present the design equations for the coefficients of Eqs. (18) in the Butterworth, the two Chebyshev, and the elliptic cases.

2. Butterworth Designs

Using Eq. (93) for the Butterworth zeros and poles, we obtain the following expression for the analog transfer function (18a) in the Butterworth case:

$$H_a(s) = \left[\frac{g\beta + g_0s}{\beta + s} \right]^r \prod_{i=1}^L \left[\frac{g^2\beta^2 + 2gg_0s_i\beta s + g_0^2s^2}{\beta^2 + 2s_i\beta s + s^2} \right] \quad (19)$$

where we defined the parameters:

$$g = G^{1/N}, \quad g_0 = G_0^{1/N}, \quad \beta = \varepsilon^{-1/N} \Omega_B = \varepsilon^{-1/N} \tan\left(\frac{\Delta\omega}{2}\right) \quad (20)$$

$$s_i = \sin \phi_i, \quad \phi_i = \frac{(2i-1)\pi}{2N}, \quad i = 1, 2, \dots, L \quad (21)$$

The parameter ε is given by Eq. (12) and Ω_B by Eq. (5). Using the coefficient transformations given in Appendix A.1, we find the coefficients of the digital lowpass shelving filter (18b):

$$\begin{aligned} D_0 &= \beta + 1 & D_i &= \beta^2 + 2s_i\beta + 1 \\ \hat{b}_{00} &= (g\beta + g_0)/D_0 & \hat{b}_{i0} &= (g^2\beta^2 + 2gg_0s_i\beta + g_0^2)/D_i \\ \hat{b}_{01} &= (g\beta - g_0)/D_0 & \hat{b}_{i1} &= 2(g^2\beta^2 - g_0^2)/D_i \\ \hat{a}_{01} &= (\beta - 1)/D_0 & \hat{b}_{i2} &= (g^2\beta^2 - 2gg_0s_i\beta + g_0^2)/D_i \\ & & \hat{a}_{i1} &= 2(\beta^2 - 1)/D_i \\ & & \hat{a}_{i2} &= (\beta^2 - 2s_i\beta + 1)/D_i \end{aligned} \quad (22)$$

The coefficients of the second and fourth-order sections of the bandpass equalizer (18c) are:

$$\begin{aligned} D_0 &= \beta + 1 & D_i &= \beta^2 + 2s_i\beta + 1 \\ b_{00} &= (g_0 + g\beta)/D_0 & b_{i0} &= (g^2\beta^2 + 2gg_0s_i\beta + g_0^2)/D_i \\ b_{01} &= -2g_0c_0/D_0 & b_{i1} &= -4c_0(g_0^2 + gg_0s_i\beta)/D_i \\ b_{02} &= (g_0 - g\beta)/D_0 & b_{i2} &= 2(g_0^2(1 + 2c_0^2) - g^2\beta^2)/D_i \\ a_{01} &= -2c_0/D_0 & b_{i3} &= -4c_0(g_0^2 - gg_0s_i\beta)/D_i \\ a_{02} &= (1 - \beta)/D_0 & b_{i4} &= (g^2\beta^2 - 2gg_0s_i\beta + g_0^2)/D_i \\ & & a_{i1} &= -4c_0(1 + s_i\beta)/D_i \\ & & a_{i2} &= 2(1 + 2c_0^2 - \beta^2)/D_i \\ & & a_{i3} &= -4c_0(1 - s_i\beta)/D_i \\ & & a_{i4} &= (\beta^2 - 2s_i\beta + 1)/D_i \end{aligned} \quad (23)$$

When $N = 1$, we have $g = G$, $g_0 = G_0$, $\beta = \varepsilon^{-1} \tan(\Delta\omega/2)$, and the second-order section coefficients $\{b_{00}, b_{01}, b_{02}, a_{01}, a_{02}\}$ become identical to those of the conventional biquadratic equalizer, for example, in the form given in [13,14]. The $N = 2$ case corresponds to the second-order shelving filters discussed in [3,12] and used in [18] to design a fourth-order equalizer. We note also that Eqs. (19)-(23) have the proper limits in the ordinary resonator/bandpass and notch/bandstop cases $G_0 = 0, G = 1$ and $G_0 = 1, G = 0$.

3. Chebyshev Type-1 Designs

For the Chebyshev designs, the bandwidth $\Delta\omega$ and gain level G_B define the extent of the equiripple passband in the type-1 case, or the onset of the equiripple stopband in the type-2 case.

Therefore, for the type-1 case, G_B must be chosen to be very close to G in order to achieve a flat passband, and for the type-2 case, it must be very close to G_0 to achieve a flat stopband. These remarks are illustrated in Fig. 2.

For the type-1 case, the analog zeros and poles are given by Eq. (96) of Appendix A.2. The resulting analog transfer function takes the form:

$$H_a(s) = \left[\frac{b\Omega_B + g_0 s}{a\Omega_B + s} \right]^r \prod_{i=1}^L \left[\frac{(b^2 + g_0^2 c_i^2) \Omega_B^2 + 2g_0 b s_i \Omega_B s + g_0^2 s^2}{(a^2 + c_i^2) \Omega_B^2 + 2a s_i \Omega_B s + s^2} \right] \quad (24)$$

where we defined $g_0 = G_0^{1/N}$ and:

$$b = g_0 \sinh u = \frac{1}{2} (\beta - g_0^2 \beta^{-1}), \quad a = \sinh v = \frac{1}{2} (\alpha - \alpha^{-1}) \quad (25)$$

$$e^u = g_0^{-1} \beta, \quad \beta = (G\varepsilon^{-1} + G_B \sqrt{1 + \varepsilon^{-2}})^{1/N}, \quad e^v = \alpha = (\varepsilon^{-1} + \sqrt{1 + \varepsilon^{-2}})^{1/N} \quad (26)$$

$$s_i = \sin \phi_i, \quad c_i = \cos \phi_i, \quad \phi_i = \frac{(2i-1)\pi}{2N}, \quad i = 1, 2, \dots, L \quad (27)$$

The choice of these parameters allows a graceful passage to the limit $G_0 = 0$, $G = 1$, which is relevant in designing ordinary lowpass and bandpass filters. Using Eq. (89) of Appendix A.1, the digital lowpass shelving filter coefficients of Eq. (18b) are found to be:

$$\begin{aligned} D_0 &= a\Omega_B + 1 & D_i &= (a^2 + c_i^2) \Omega_B^2 + 2a s_i \Omega_B + 1 \\ \hat{b}_{00} &= (b\Omega_B + g_0) / D_0 & \hat{b}_{i0} &= ((b^2 + g_0^2 c_i^2) \Omega_B^2 + 2g_0 b s_i \Omega_B + g_0^2) / D_i \\ \hat{b}_{01} &= (b\Omega_B - g_0) / D_0 & \hat{b}_{i1} &= 2((b^2 + g_0^2 c_i^2) \Omega_B^2 - g_0^2) / D_i \\ \hat{a}_{01} &= (a\Omega_B - 1) / D_0 & \hat{b}_{i2} &= ((b^2 + g_0^2 c_i^2) \Omega_B^2 - 2g_0 b s_i \Omega_B + g_0^2) / D_i \\ & & \hat{a}_{i1} &= 2((a^2 + c_i^2) \Omega_B^2 - 1) / D_i \\ & & \hat{a}_{i2} &= ((a^2 + c_i^2) \Omega_B^2 - 2a s_i \Omega_B + 1) / D_i \end{aligned} \quad (28)$$

and using Eq. (90), we obtain the bandpass equalizer coefficients:

$$\begin{aligned} D_0 &= a\Omega_B + 1 & D_i &= (a^2 + c_i^2) \Omega_B^2 + 2a s_i \Omega_B + 1 \\ b_{00} &= (g_0 + b\Omega_B) / D_0 & b_{i0} &= ((b^2 + g_0^2 c_i^2) \Omega_B^2 + 2g_0 b s_i \Omega_B + g_0^2) / D_i \\ b_{01} &= -2g_0 c_0 / D_0 & b_{i1} &= -4c_0 (g_0^2 + g_0 b s_i \Omega_B) / D_i \\ b_{02} &= (g_0 - b\Omega_B) / D_0 & b_{i2} &= 2(g_0^2 (1 + 2c_0^2) - (b^2 + g_0^2 c_i^2) \Omega_B^2) / D_i \\ a_{01} &= -2c_0 / D_0 & b_{i3} &= -4c_0 (g_0^2 - g_0 b s_i \Omega_B) / D_i \\ a_{02} &= (1 - a\Omega_B) / D_0 & b_{i4} &= ((b^2 + g_0^2 c_i^2) \Omega_B^2 - 2g_0 b s_i \Omega_B + g_0^2) / D_i \\ & & a_{i1} &= -4c_0 (1 + a s_i \Omega_B) / D_i \\ & & a_{i2} &= 2(1 + 2c_0^2 - (a^2 + c_i^2) \Omega_B^2) / D_i \\ & & a_{i3} &= -4c_0 (1 - a s_i \Omega_B) / D_i \\ & & a_{i4} &= ((a^2 + c_i^2) \Omega_B^2 - 2a s_i \Omega_B + 1) / D_i \end{aligned} \quad (29)$$

4. Chebyshev Type-2 Designs

In the type-2 Chebyshev case, the analog shelving filter transfer function of Eq. (18a), constructed from the corresponding left-hand s -plane zeros and poles given by Eq. (98), is found to be:

$$H_a(s) = \left[\frac{g\Omega_B + bs}{\Omega_B + as} \right]^r \prod_{i=1}^L \left[\frac{g^2\Omega_B^2 + 2gbs_i\Omega_Bs + (b^2 + g^2c_i^2)s^2}{\Omega_B^2 + 2as_i\Omega_Bs + (a^2 + c_i^2)s^2} \right] \quad (30)$$

where we set $g = G^{1/N}$ and defined:

$$b = g \sinh u = \frac{1}{2}(\beta - g^2\beta^{-1}), \quad a = \sinh v = \frac{1}{2}(\alpha - \alpha^{-1}) \quad (31)$$

with s_i, c_i, ϕ_i given by Eq. (27), and the quantities u, v defined by:

$$e^u = g^{-1}\beta, \quad \beta = (G_0\varepsilon + G_B\sqrt{1 + \varepsilon^2})^{1/N}, \quad e^v = \alpha = (\varepsilon + \sqrt{1 + \varepsilon^2})^{1/N} \quad (32)$$

The form of Eq. (30) facilitates the limit $G = 0, G_0 = 1$, which describes ordinary notch/bandstop filters. The coefficients of the corresponding digital lowpass shelving filter are:

$$\begin{aligned} D_0 &= \Omega_B + a & D_i &= \Omega_B^2 + 2as_i\Omega_B + a^2 + c_i^2 \\ \hat{b}_{00} &= (g\Omega_B + b)/D_0 & \hat{b}_{i0} &= (g^2\Omega_B^2 + 2gbs_i\Omega_B + b^2 + g^2c_i^2)/D_i \\ \hat{b}_{01} &= (g\Omega_B - b)/D_0 & \hat{b}_{i1} &= 2(g^2\Omega_B^2 - b^2 - g^2c_i^2)/D_i \\ \hat{a}_{01} &= (\Omega_B - a)/D_0 & \hat{b}_{i2} &= (g^2\Omega_B^2 - 2gbs_i\Omega_B + b^2 + g^2c_i^2)/D_i \\ & & \hat{a}_{i1} &= 2(\Omega_B^2 - a^2 - c_i^2)/D_i \\ & & \hat{a}_{i2} &= (\Omega_B^2 - 2as_i\Omega_B + a^2 + c_i^2)/D_i \end{aligned} \quad (33)$$

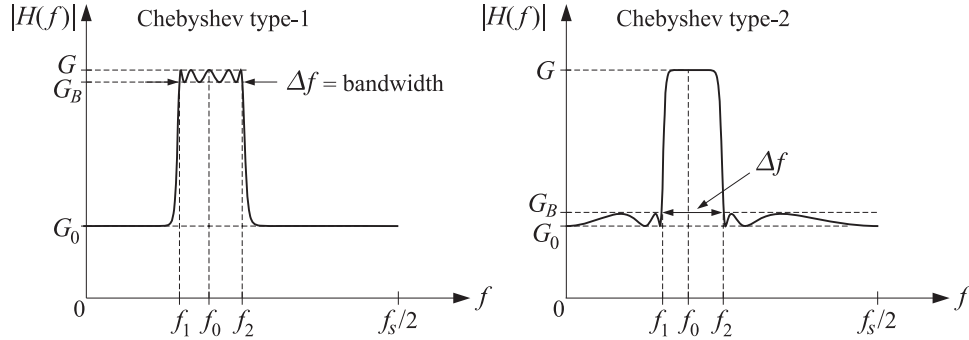


Fig. 2 Bandwidth specifications of Chebyshev type-1 and type-2 equalizers.

and the coefficients of the bandpass equalizer:

$$\begin{aligned}
D_0 &= \Omega_B + a & D_i &= \Omega_B^2 + 2as_i\Omega_B + a^2 + c_i^2 \\
b_{00} &= (b + g\Omega_B)/D_0 & b_{i0} &= (g^2\Omega_B^2 + 2gbs_i\Omega_B + b^2 + g^2c_i^2)/D_i \\
b_{01} &= -2bc_0/D_0 & b_{i1} &= -4c_0(b^2 + g^2c_i^2 + gbs_i\Omega_B)/D_i \\
b_{02} &= (b - g\Omega_B)/D_0 & b_{i2} &= 2((b^2 + g^2c_i^2)(1 + 2c_0^2) - g^2\Omega_B^2)/D_i \\
a_{01} &= -2ac_0/D_0 & b_{i3} &= -4c_0(b^2 + g^2c_i^2 - gbs_i\Omega_B)/D_i \\
a_{02} &= (a - \Omega_B)/D_0 & b_{i4} &= (g^2\Omega_B^2 - 2gbs_i\Omega_B + b^2 + g^2c_i^2)/D_i \\
& & a_{i1} &= -4c_0(a^2 + c_i^2 + as_i\Omega_B)/D_i \\
& & a_{i2} &= 2((a^2 + c_i^2)(1 + 2c_0^2) - \Omega_B^2)/D_i \\
& & a_{i3} &= -4c_0(a^2 + s_i^2 - as_i\Omega_B)/D_i \\
& & a_{i4} &= (\Omega_B^2 - 2as_i\Omega_B + a^2 + c_i^2)/D_i
\end{aligned} \tag{34}$$

We note that for both Chebyshev cases, the filter order $N = 1$ corresponds to the conventional biquadratic equalizer.

5. Elliptic Designs

In this section we adapt the conventional elliptic filter design methods [22-27] to the equalizer problem. We follow the notational conventions and computational algorithms of Ref. [25]. The required elliptic function moduli k, k_1 may be determined in terms of the given filter specifications by the procedure described below.

The use of the elliptic function cd (instead of usual sn) in the definition of Eq. (11) applies to both the even and odd values of the filter order N . The elliptic function moduli k, k_1 and the filter order N are required to satisfy the following "degree equation":

$$N \frac{K'}{K} = \frac{K'_1}{K_1} \tag{35}$$

where K, K' and K_1, K'_1 are the quarter periods corresponding to the moduli k, k_1 and defined in terms of the complete elliptic integrals [29-31] by $K = K(k)$, $K' = K(k')$, $K_1 = K(k_1)$, and $K'_1 = K(k'_1)$, where k', k'_1 are the complementary moduli $k' = (1 - k^2)^{1/2}$ and $k'_1 = (1 - k_1^2)^{1/2}$.

A consequence of the degree equation [23,27] is that $F_N(w) = \text{cd}(NuK_1, k_1)$ is a rational function of $w = \text{cd}(uK, k)$ given as follows (and normalized such that $F_N(1) = 1$):

$$F_N(w) = [w]^r \prod_{i=1}^L \left[\left(\frac{w^2 - \zeta_i^2}{1 - w^2 k^2 \zeta_i^2} \right) \left(\frac{1 - k^2 \zeta_i^2}{1 - \zeta_i^2} \right) \right] \tag{36}$$

where $N = 2L + r$, and ζ_i and $(k\zeta_i)^{-1}$ are the zeros and poles of $F_N(w)$, where:

$$\zeta_i = \text{cd}(u_i K, k), \quad u_i = \frac{2i - 1}{N}, \quad i = 1, 2, \dots, L \tag{37}$$

Because the elliptic designs are equiripple in both the passband and stopband, the specifications of the equalizer must be modified by adding a gain G_s that defines the level of the

equiripple stopband. These specifications and those of the equivalent analog lowpass shelving filter are shown in Fig. 3.

The gain G_B defines the equiripple passband, which extends over the $\pm\Omega_B$ interval for the shelving filter. The equiripple stopband begins at a frequency $\Omega_s > \Omega_B$ that defines the elliptic modulus $k = \Omega_B/\Omega_s$. At the normalized frequency $w_1 = \Omega_s/\Omega_B = 1/k$, we have $F_N(w_1) = 1/k_1$. Indeed, the condition that $w_1 = \text{cd}(uK, k) = 1/k$ is satisfied with $u = jK'/K$, that is, $\text{cd}(uK, k) = \text{cd}(jK', k) = 1/k$, which is a standard property of the cd elliptic function [30,31]. Then, the same property and the degree equation (35) imply that:

$$F_N(w_1) = \text{cd}(NuK_1, k_1) = \text{cd}(jNK_1K'/K, k_1) = \text{cd}(jK'_1, k_1) = 1/k_1 \quad (38)$$

Using Eq. (38), the requirement that the gain be equal to G_s at $w = w_1$ gives the condition:

$$|H_a(\Omega_s)|^2 = \frac{G^2 + G_0^2 \varepsilon^2 / k_1^2}{1 + \varepsilon^2 / k_1^2} = G_s^2 \Leftrightarrow k_1 = \frac{\varepsilon}{\varepsilon_s}, \quad \varepsilon_s = \sqrt{\frac{G^2 - G_s^2}{G_s^2 - G_0^2}} \quad (39)$$

Thus, the elliptic moduli k, k_1 are given as follows in terms of the shelving filter specifications:

$$k = \frac{\Omega_B}{\Omega_s}, \quad k_1 = \frac{\varepsilon}{\varepsilon_s} \quad (40)$$

Because of the degree equation, any two of the parameters N, G_s, Ω_s , or equivalently, N, k, k_1 , will determine the third. For the equalizer problem, it is convenient to fix N and G_s , with G_s chosen to be very close to G_0 in order to achieve a flat stopband. Then, from the degree equation we may determine the parameter k and, hence, the value of the stopband edge frequency Ω_s .

An exact solution of the degree equation can be derived by using the property of Eq. (38). Setting $w_1 = 1/k$ and $F_N(w_1) = 1/k_1$ in Eq. (36), we obtain the formula for k_1 :

$$k_1 = k^N \prod_{i=1}^L \text{sn}^4(u_i K, k) \quad (41)$$

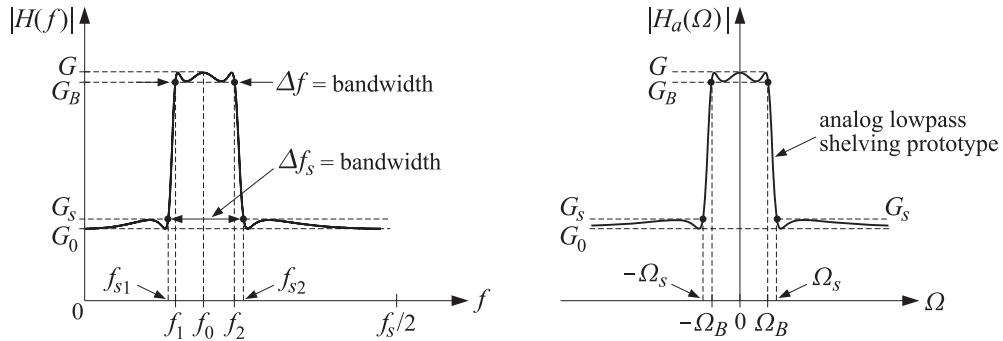


Fig. 3 Design specifications of elliptic equalizer and corresponding shelving filter.

where we used the property: $(1 - \zeta_i^2)/(1 - k^2\zeta_i^2) = \text{sn}^2(u_iK, k)$. Noting the invariance [28] of the degree equation under the substitutions $k \rightarrow k'_1$ and $k_1 \rightarrow k'$, we also obtain the exact solution for k in terms of N, k_1 , expressed via the complementary moduli k', k'_1 :

$$k' = (k'_1)^N \prod_{i=1}^L \text{sn}^4(u_iK'_1, k'_1) \quad (42)$$

Eqs. (41) and (42), known as the “modular equations,” were derived first by Jacobi in his original treatise on elliptic functions [29] and have been used since in the context of elliptic filter design [23,27,28].

The degree equation can also be solved approximately, and accurately, by working with the nomos q, q_1 corresponding to the moduli k, k_1 . Exponentiating Eq. (35), we have:

$$q_1 = q^N \Leftrightarrow q = q_1^{1/N} \quad (43)$$

where $q = e^{-\pi K'/K}$ and $q_1 = e^{-\pi K'_1/K_1}$. Once q has been calculated from N and q_1 , the modulus k can be determined from the series expansion [30]:

$$k = 4\sqrt{q} \left(\frac{\sum_{m=0}^{\infty} q^{m(m+1)}}{1 + 2 \sum_{m=1}^{\infty} q^{m^2}} \right)^2 \quad (44)$$

which converges very fast. For example, keeping only the terms up to $m = 7$, gives a very accurate approximation.

The shelving filter transfer function $H_a(s)$ is constructed by Eq. (13), where the poles p_0, p_i are given by Eqs. (100)–(102) of Appendix A.2 and the zeros z_0, z_i by Eqs. (104)–(105). The expressions for the zeros take into account the special cases $G = 1, G_0 = 0$ and $G = 0, G_0 = 1$.

Once $H_a(s)$ is determined from its zeros and poles, it may be transformed to the digital equalizer forms of Eq. (18) using the bilinear transformations. The required coefficient transformations are given by Eqs. (89) and (90) of Appendix A.1. The resulting digital filter coefficients do not have any easily stated analytical form. They have been implemented numerically by the MATLAB functions of Appendix A.6.

From the calculated value of $\Omega_s = \Omega_B/k$, the equalizer’s bandwidth, $\Delta\omega_s = 2\pi\Delta f_s/f_s$, at the stopband level G_s can be derived by inverting the relationship $\Omega_s = \tan(\Delta\omega_s/2)$. The left and right stopband edge frequencies can be calculated from Eq. (8) with Ω_s replacing Ω_B :

$$\cos \omega_{s1} = \frac{c_0 + \Omega_s \sqrt{\Omega_s^2 + s_0^2}}{\Omega_s^2 + 1}, \quad \cos \omega_{s2} = \frac{c_0 - \Omega_s \sqrt{\Omega_s^2 + s_0^2}}{\Omega_s^2 + 1} \quad (45)$$

We note that the type-1 Chebyshev designs correspond to the limit $\Omega_s \rightarrow \infty, G_s \rightarrow G_0$, or, $k = k_1 = 0$. In this limit, the quarter periods become $K = K_1 = \pi/2$, the elliptic function cd tends to an ordinary cosine, $w = \text{cd}(uK, k) = \cos(u\pi/2)$, and the function $F_N(w) = \text{cd}(NuK_1, k_1) = \cos(Nu\pi/2)$ becomes equal to the N th order Chebyshev polynomial $C_N(w)$, and the $\zeta_i = \text{cd}(u_iK, k) = \cos(u_i\pi/2)$ become its roots.

6. Order Determination

We saw in the elliptic case that the order N and the stopband level G_s were enough to fix the rest of the design parameters, and in particular, the bandwidth Δf_s at G_s . Conversely, if Δf , Δf_s and the levels G_B , G_s are specified independently, then, the moduli k, k_1 are fixed and may not necessarily satisfy the degree equation (35) with an integer N . In this case, one may calculate:

$$N = \frac{K'_1/K_1}{K'/K} \quad (46)$$

and round it up to the next integer. Then, either k_1 needs to be recalculated from Eq. (41), or k from Eq. (42). Given that N is a decreasing function of k_1 and an increasing function of k , it follows that the resulting specifications will be slightly improved. In the first case, k_1 will slightly decrease implying that either ε decreases or ε_s increases, and hence, either G_B gets closer to G , or G_s gets closer to G_0 . In the second case, k will slightly increase, implying that Ω_s will get smaller, resulting in a narrower bandwidth Δf_s .

A similar determination of the order N can be carried out in the Butterworth and Chebyshev cases. One must specify a secondary bandwidth specification, such as Δf_s at G_s , as illustrated in Fig. 3. Defining the parameters k, k_1 exactly as in Eq. (40), and using the condition that $F_N(w_1) = 1/k_1$ at $w_1 = 1/k$, we obtain the following degree equations. For the Butterworth case:

$$k_1 = k^N \quad \Rightarrow \quad N = \frac{\ln k_1}{\ln k} \quad (47)$$

For the type-1 Chebyshev case, we have $C_N(1/k) = 1/k_1$, or,

$$\cosh(N \cosh^{-1}(1/k)) = 1/k_1 \quad \Rightarrow \quad N = \frac{\cosh^{-1}(1/k_1)}{\cosh^{-1}(1/k)} \quad (48)$$

For the type-2 Chebyshev case, because G_B was chosen to be close to G_0 , the secondary bandwidth level G_s must be chosen to be very close to G , thus corresponding to a narrower bandwidth Δf_s than Δf . This implies that $k = \Omega_B/\Omega_s > 1$ and also $k_1 = \varepsilon/\varepsilon_s > 1$. The degree equation in this case is $C_N(k) = k_1$, or,

$$\cosh(N \cosh^{-1} k) = k_1 \quad \Rightarrow \quad N = \frac{\cosh^{-1} k_1}{\cosh^{-1} k} \quad (49)$$

The inequality $\varepsilon_s < \varepsilon$ for the type-2 case can be seen from the identity:

$$\varepsilon_s^2 - \varepsilon^2 = \frac{(G_B^2 - G_s^2)(G^2 - G_0^2)}{(G_s^2 - G_0^2)(G_B^2 - G_0^2)} \quad (50)$$

where for a boost, we must have $G > G_s > G_B > G_0$, and for a cut, $G < G_s < G_B < G_0$. For the Butterworth, type-1 Chebyshev, and elliptic cases, we always have $\varepsilon_s > \varepsilon$, because for a boost we must have $G > G_B > G_s > G_0$, and for a cut, $G < G_B < G_s < G_0$.

7. Bandwidth

The bandwidth levels G_B and G_s may be chosen arbitrarily, as long as they satisfy the basic inequalities (with the roles of G_B and G_s reversed in the Chebyshev-2 case):

$$\begin{aligned} G &> G_B > G_s > G_0 \quad (\text{boost}) \\ G &< G_B < G_s < G_0 \quad (\text{cut}) \end{aligned} \quad (51)$$

If the boost gain is more than 3 dB above the reference G_0 , one may choose G_B to be 3 dB below the peak, $G_B^2 = G^2/2$, or, alternatively, 3 dB above the reference, $G_B^2 = 2G_0^2$. Other choices that respect the inequalities (51) are the geometric and arithmetic means [14]:

$$G_B^2 = GG_0, \quad G_B^2 = \frac{1}{2}(G^2 + G_0^2) \quad (52)$$

The corresponding values of ε defined by Eq. (12) are in these cases:

$$\varepsilon = \sqrt{\frac{G}{G_0}}, \quad \varepsilon = 1 \quad (53)$$

A more general definition is the weighted arithmetic mean:

$$G_B^2 = \frac{G^2 + \alpha^2 G_0^2}{1 + \alpha^2} \Rightarrow \varepsilon = \alpha \quad (54)$$

where α is an arbitrary constant. The geometric mean choice implies that a boost and a cut by equal and opposite gains in dB will cancel exactly [9]. On the other hand, as we discuss in the next section, the weighted arithmetic mean makes possible a generalization of the Regalia-Mitra realization [5] that allows the independent control of the filter coefficients by the equalizer's center frequency f_0 , bandwidth Δf , and gain G .

Regardless of the choice of G_B , and for all four filter types, it can be shown that a boost and a cut by gains G and G^{-1} , with bandwidth levels G_B and G_B^{-1} , and with the same center frequency and bandwidth, will cancel each other. Consider the boost and the cut defined by the gains:

$$\begin{aligned} G &> G_B > G_s > G_0 \quad (\text{boost}) \\ G^{-1} &< G_B^{-1} < G_s^{-1} < G_0^{-1} \quad (\text{cut}) \end{aligned} \quad (55)$$

From the definition (12), it follows that:

$$\varepsilon_{\text{cut}} = \sqrt{\frac{G^{-2} - G_B^{-2}}{G_B^{-2} - G_0^{-2}}} = \frac{G_0}{G} \sqrt{\frac{G^2 - G_B^2}{G_B^2 - G_0^2}} = \frac{G_0}{G} \varepsilon_{\text{boost}} \quad (56)$$

This implies that the root conditions (92) for the zeros and poles will exchange roles, and therefore, $z_{i,\text{cut}} = p_{i,\text{boost}}$ and $p_{i,\text{cut}} = z_{i,\text{boost}}$. The corresponding analog, and hence, the digital transfer functions will become inverses of each other:

$$H_{\text{cut}}(z) = \frac{1}{H_{\text{boost}}(z)} \quad (57)$$

The elliptic modulus k_1 remains invariant under this change because the quantity ε_s also changes in the same way as in Eq. (56), and therefore, the ratio $\varepsilon/\varepsilon_s$ remains unchanged.

The bandwidth $\Delta\omega = \omega_2 - \omega_1$ is given in linear frequency scale and enters the design equations, for all filter types, through the quantity $\Omega_B = \tan(\Delta\omega/2)$. If the bandwidth is to be specified in octaves, then it may be mapped to the linear $\Delta\omega$ in the following way.

Because the quantities $\Omega_i = \tan(\omega_i/2)$, $i = 0, 1, 2$, are related through $\Omega_1\Omega_2 = \Omega_0^2$, that is, through Eq. (5), we may set $\Omega_2 = 2^{B/2}\Omega_0$ and $\Omega_1 = 2^{-B/2}\Omega_0$, where B plays the role of an equivalent analog octave bandwidth. Using some trigonometric identities, we obtain the following expression for $\Delta\omega$ in terms of B :

$$\Omega_B = \tan\left(\frac{\Delta\omega}{2}\right) = \sin\omega_0 \sinh\left(\frac{\ln 2}{2} B\right) \quad (58)$$

The true bandwidth in octaves is defined by $b = \log_2(\omega_2/\omega_1)$, or, $2^b = \omega_2/\omega_1$. Replacing $\omega_2 = 2 \arctan(\Omega_2) = 2 \arctan(2^{B/2}\Omega_0)$, and similarly for ω_1 , we obtain the following “bandwidth equation” relating B , b , and $\Omega_0 = \tan(\omega_0/2)$ [32]:

$$2^b = \frac{\arctan(2^{B/2}\Omega_0)}{\arctan(2^{-B/2}\Omega_0)} \quad (59)$$

In order to map the given octave bandwidth b to the linear one, one must solve Eq. (59) for B and substitute it in (58). By expanding (59) to first order in b and B , Bristow-Johnson obtained the following approximate solution [9]:

$$B = \frac{\omega_0}{\sin\omega_0} b \quad (60)$$

This approximation works very well for low frequencies ω_0 , as well as for high ω_0 and narrow b . For any values of ω_0 and b , Eq. (59) may be solved iteratively, with Eq. (60) serving as the starting point. By rearranging (59) in the form $2^{B/2} = \Omega_0 / \tan(2^{-b} \arctan(2^{B/2}\Omega_0))$, we obtain the following convergent iteration, initialized at $B_0 = B$ given by (60):

$$2^{B_{n+1}/2} = \frac{\Omega_0}{\tan(2^{-b} \arctan(2^{B_n/2}\Omega_0))}, \quad n = 0, 1, 2, \dots \quad (61)$$

At large values of ω_0 where the approximation (60) is not as good, the convergence is very fast, requiring only two or three iterations; the convergence is slow at small ω_0 , but then the approximation (60) is good and there is no need for the iteration. The calculated physical bandwidth at the n th iteration may be defined through $2^{b_n} = \arctan(2^{B_n/2}\Omega_0) / \arctan(2^{-B_n/2}\Omega_0)$. The iteration error $|b_n - b|$ decreases essentially exponentially with the iteration index n . This can be seen as follows. Assuming that B_n is near the desired solution B of (59), and linearizing the recursion (61) about B , we obtain the following solution for the errors $\Delta B_n = B_n - B$:

$$\Delta B_n = \text{const} \cdot (-a)^n, \quad a = \frac{(2^B + \Omega_0^2) \arctan(2^{-B/2}\Omega_0)}{(1 + 2^B \Omega_0^2) \arctan(2^{B/2}\Omega_0)} \quad (62)$$

where the quantity a can be shown to be less than unity for all values of B and Ω_0 , and a decreasing function of B ($a \lesssim 1$ at low ω_0 , which explains the slow convergence in that case.) Thus, ΔB_n decreases exponentially, and so does the error $|b_n - b|$, since it follows $|\Delta B_n|$.

Once B has been calculated from b and ω_0 , it may be used in (58) to obtain the linear bandwidth $\Delta\omega$ and, from it, the actual bandedge frequencies ω_1, ω_2 through Eqs. (8), or from $\omega_{2,1} = 2 \arctan(2^{\pm B/2} \Omega_0)$. The calculated bandedge frequencies will always lie within the Nyquist interval, for all values of ω_0 and b . However, it must be emphasized that, although ω_1, ω_2 are b -octaves apart, they will not necessarily lie symmetrically at $\pm b/2$ octaves about ω_0 , and may result in a very asymmetric band, especially at large ω_0 s.

For the Chebyshev and elliptic cases, it may be desirable to be able to design the filters based on a more standard definition of the bandwidth, such as the 3-dB width, yet preserving the flatness of the passband and stopband controlled by the gains G_B and G_s . This issue has been discussed in [33]. In general terms, the problem is to compute the design bandwidth $\Delta\omega$ at the level G_B from a given bandwidth $\Delta\omega_b$ at an arbitrary intermediate level G_b , such that $G_0 < G_s < G_b < G_B < G$. For a given order N , the required bandwidth $\Delta\omega$ and the design parameter Ω_B can be determined from $\Delta\omega_b$ as follows:

$$\Omega_B = \tan\left(\frac{\Delta\omega}{2}\right) = \frac{1}{w_b} \tan\left(\frac{\Delta\omega_b}{2}\right) \quad (63)$$

where the normalized frequency w_b is the solution of the equation:

$$F_N(w_b) = \frac{\varepsilon_b}{\varepsilon}, \quad \varepsilon_b = \sqrt{\frac{G^2 - G_b^2}{G_b^2 - G_0^2}} \quad (64)$$

Eq. (64) was obtained from the equivalent magnitude condition:

$$\frac{G^2 + G_0^2 \varepsilon^2 F_N^2(w_b)}{1 + \varepsilon^2 F_N^2(w_b)} = G_b^2 \quad (65)$$

The solution of (64) is straightforward. For example, for the type-1 Chebyshev case, one may solve $\cosh(Nu) = \varepsilon_b/\varepsilon$ for u and then calculate $w_b = \cosh(u)$. Similarly, for the elliptic case, using the inverse of the cd elliptic function (see Appendix A.3), one may solve $\text{cd}(NuK_1, k_1) = \varepsilon_b/\varepsilon$ for u and compute $w_b = \text{cd}(uK, k)$, where k_1 is fixed from the levels G_B and G_s , and k is calculated from N, k_1 using the degree equation. Once the bandwidth $\Delta\omega$ is determined, it may be used to complete the filter design. If the G_b -bandwidth is given in octaves, then it can be converted to linear frequency scale by applying Eqs. (58)–(61) to $\Delta\omega_b$ instead of $\Delta\omega$.

If the filter order N is not given, but rather both $\Delta\omega, \Delta\omega_b$ at the levels G_B, G_b are given, then, the quantities ε_b and $w_b = \tan(\Delta\omega_b/2) / \tan(\Delta\omega/2)$ are fixed and the filter order may be determined by solving Eq. (64) for N as in Sect. 6. This is straightforward for the Butterworth and Chebyshev cases.

The elliptic case is a bit more difficult because the third level G_s must also be fixed independently. The following trial-and-error approach works well: for each successive filter order $N = 1, 2, \dots$, calculate k from N, k_1 using the degree equation, then solve $\text{cd}(NuK_1, k_1) = \varepsilon_b/\varepsilon$ for u , calculate the error $e = \text{cd}(uK, k) - w_b$, and keep the first N for which e becomes negative (it always starts from positive values provided that $w_b < \varepsilon_b/\varepsilon$, which is easily met for practical specifications.)

If the filter is designed with the computed N and the given $\Delta\omega$, then the resulting G_b -width will be slightly narrower than $\Delta\omega_b$. If the width $\Delta\omega_b$ is to be matched exactly, the resulting $\Delta\omega$, obtained from Eqs. (63)–(64) using the computed N , will be slightly wider than specified. All of the above operations can be implemented by the MATLAB functions of Appendix A.6.

8. Realizations

The digital equalizer transfer function $H(z)$ given by Eq. (18) may be realized as the cascade of the fourth-order sections in (18c), or alternatively, as the cascade of the frequency-shifted second-order lowpass shelving filter sections in (18b), in which each unit delay \hat{z}^{-1} is replaced by the lowpass to bandpass transformation of Eq. (17).

We consider briefly the frequency-shifted versions of the transposed, normalized-lattice [34–36], and minimum-noise state-space [37–41] realizations of Eq. (18b). The latter two are known to have excellent numerical properties, at the expense of effectively doubling the number of filter coefficients. Such realizations may be appropriate under stringent filter specifications, such as very low center frequencies or rapidly-varying equalizer parameters [36].

The normalized lattice realization of the transformation (17) is shown in Fig. 4. It has the expected limit (without requiring any pole/zero cancellations) in the lowpass and highpass shelving filter cases $\omega_0 = 0$ and $\omega_0 = \pi$. Other realizations of (17) are, of course, possible that require fewer operations, such as, for example, the one-multiplier form of [8,21]. However, they lack the scaling and L_2 -normalization properties of the normalized lattice.

The transposed (of the direct-form II) realization of the second-order sections of Eq. (18b), after each delay \hat{z}^{-1} has been replaced by Fig. 4, is shown in Fig. 5. The figure represents the transfer function:

$$\frac{B(\hat{z})}{A(\hat{z})} = \frac{\hat{b}_0 + \hat{b}_1\hat{z}^{-1} + \hat{b}_2\hat{z}^{-2}}{1 + \hat{a}_1\hat{z}^{-1} + \hat{a}_2\hat{z}^{-2}}, \quad \hat{z}^{-1} = \frac{(c_0 - z^{-1})z^{-1}}{1 - c_0z^{-1}} \quad (66)$$

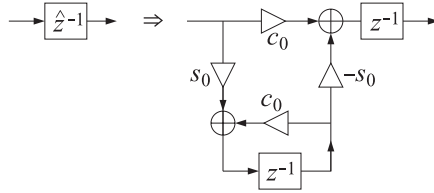


Fig. 4 Normalized lattice realization of Eq. (17).

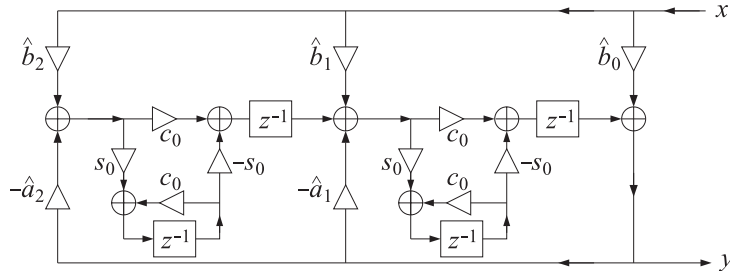


Fig. 5 Frequency-shifted transposed realization of the filter sections of Eq. (18b).

The normalized lattice realization of Eq. (66) is shown in Fig. 6. The reflection and transmission coefficients are constructed as follows [34–36]:

$$y_1 = \frac{\hat{a}_1}{1 + \hat{a}_2}, \quad y_2 = \hat{a}_2, \quad \tau_1 = \sqrt{1 - y_1^2}, \quad \tau_2 = \sqrt{1 - y_2^2} \quad (67)$$

The ladder coefficients d_0, d_1, d_2 are the solutions of the triangular system:

$$\begin{bmatrix} 1 & y_1 & \hat{a}_2 \\ 0 & 1 & \hat{a}_1 \\ 0 & 0 & 1 \end{bmatrix} \begin{bmatrix} d_0 \tau_1 \tau_2 \\ d_1 \tau_2 \\ d_2 \end{bmatrix} = \begin{bmatrix} \hat{b}_0 \\ \hat{b}_1 \\ \hat{b}_2 \end{bmatrix} \quad (68)$$

The first-order factor of Eq. (18b) is obtained by setting $\hat{a}_2 = \hat{b}_2 = 0$, or equivalently, $y_2 = 0$, $d_2 = 0$, and $\tau_2 = 1$, which amounts to deleting the y_2 lattice section.

Computationally, Eqs. (67) and (68) are simple to use. Explicit expressions for the lattice filter parameters can be given in the Butterworth and Chebyshev cases. For example, for the first-order Butterworth factor of Eq. (18b), we find:

$$y_1 = \frac{\beta - 1}{\beta + 1}, \quad d_0 = \frac{\sqrt{\beta}(g + g_0)}{\beta + 1}, \quad d_1 = \frac{g\beta - g_0}{\beta + 1} \quad (69)$$

Eq. (69) can also be used to implement the conventional biquadratic equalizer. For the i th second-order Butterworth factor of (18b), we have:

$$y_1 = \frac{\beta^2 - 1}{\beta^2 + 1}, \quad y_2 = \frac{\beta^2 - 2s_i\beta + 1}{\beta^2 + 2s_i\beta + 1} \quad (70)$$

$$d_0 = \frac{\sqrt{\beta}(g + g_0) [(1 - \beta^2)(g - g_0) + 2s_i\beta(g + g_0)]}{(\beta^2 + 2s_i\beta + 1)\sqrt{2s_i(\beta^2 + 1)}}$$

$$d_1 = \frac{\sqrt{2\beta}(g + g_0) [g\beta(1 + \beta s_i) - g_0(\beta + s_i)]}{(\beta^2 + 2s_i\beta + 1)\sqrt{s_i(\beta^2 + 1)}} \quad (71)$$

$$d_2 = \frac{g^2\beta^2 - 2gg_0s_i\beta + g_0^2}{\beta^2 + 2s_i\beta + 1}$$

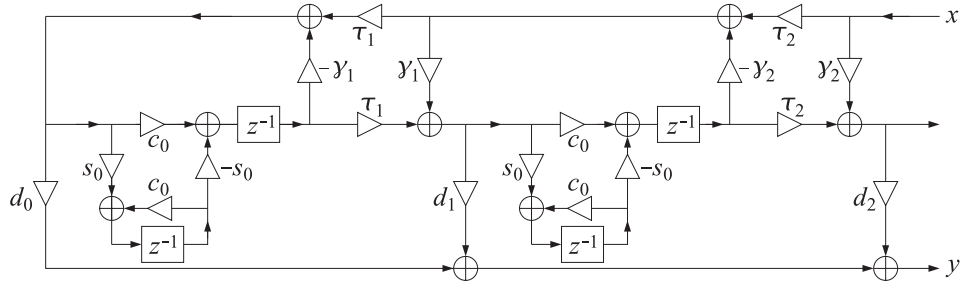


Fig. 6 Frequency-shifted normalized lattice realization of the sections of Eq. (18b).

Optimum state-space realizations that have minimum roundoff noise under fixed-point arithmetic, and under an L_2 -scaling constraint for the internal states, are well-known [37-39]. Explicit design equations for the case of second-order sections with complex-conjugate poles have been given by Barnes [40] and Bomar [41].

One may use such optimum realizations for each second-order section of Eq. (18b), and replace the delays \hat{z}^{-1} by Fig. 4. The resulting state-space realization of Eq. (66) is shown in Fig. 7, where the indicated state vectors \mathbf{s} and \mathbf{w} are two-dimensional. The corresponding time-domain description is:

$$\begin{aligned} y(n) &= \mathbf{C}\mathbf{s}(n) + D\mathbf{x}(n) \\ \mathbf{s}(n+1) &= c_0[\mathbf{A}\mathbf{s}(n) + B\mathbf{x}(n)] - s_0\mathbf{w}(n) \\ \mathbf{w}(n+1) &= s_0[\mathbf{A}\mathbf{s}(n) + B\mathbf{x}(n)] + c_0\mathbf{w}(n) \end{aligned} \quad (72)$$

The $ABCD$ parameters are given in Appendix A.4. For the odd- N case, the first-order factor in \hat{z}^{-1} is described by Eq. (72) with one-dimensional $ABCD$ parameters.

For the special case of the ordinary biquadratic equalizer ($N = 1$), the first-order factor in \hat{z}^{-1} may be regarded as a second-order factor in z^{-1} and realized directly in its optimum second-order state-space form. We have derived the following explicit form of the optimum second-order state-space parameters in this case:

$$\begin{aligned} A &= \frac{1}{1+\beta} \begin{bmatrix} c_0 & \beta + s_0 \\ \beta - s_0 & c_0 \end{bmatrix}, \quad B = \frac{\sqrt{2\beta}}{1+\beta} \begin{bmatrix} \sqrt{1-s_0} \\ -\sigma\sqrt{1+s_0} \end{bmatrix} \\ C &= \frac{\sqrt{2\beta}(G-G_0)}{2(1+\beta)} [\sigma\sqrt{1+s_0}, -\sqrt{1-s_0}], \quad D = \frac{G_0 + G\beta}{1+\beta} \end{aligned} \quad (73)$$

where $\beta = \varepsilon^{-1} \tan(\Delta\omega/2)$ and $\sigma = \text{sign}(c_0)$, with the convention that $\text{sign}(0) = 1$. The corresponding first-order lowpass and highpass shelving filters obtained in the limits $\omega_0 = 0$ and $\omega_0 = \pi$ are described by the one-dimensional state-space parameters:

$$A = \pm \frac{1-\beta}{1+\beta}, \quad B = \frac{2\sqrt{\beta}}{1+\beta}, \quad C = \pm \frac{\sqrt{\beta}(G-G_0)}{1+\beta}, \quad D = \frac{G_0 + G\beta}{1+\beta} \quad (74)$$

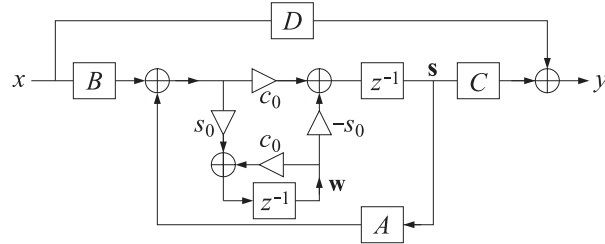


Fig. 7 Frequency-shifted state-space realization of the filter sections of Eq. (18b).

The state covariance matrix [39] of the realization (73) is found to be:

$$K = \sum_{n=0}^{\infty} A^n B B^T A^{Tn} = I \quad (75)$$

where I is the two-dimensional identity matrix. A similar result holds for the realization (74), but with I replaced by unity. We note that the L_2 -scaling rule requires that the diagonal entries of K be unity [39].

The realizations shown in Figs. 5–7 are partially decoupled in the sense that the dependence on the center frequency ω_0 resides only in the multipliers c_0, s_0 , whereas the dependence on the bandwidth and gain resides in the other coefficients.

For the Butterworth and the two Chebyshev cases, it is possible to generalize the Regalia-Mitra realizations [5] in which the dependence on the bandwidth, gain, and center frequency is completely decoupled into separate filter coefficients.

Such decoupling is possible [14] only if the bandwidth level is defined according the weighted arithmetic mean of Eq. (54). Then, the constant $\varepsilon = \alpha$ is independent of the peak gain G and hence the parameter β of Eq. (20) depends only on the bandwidth $\Delta\omega$.

For the first-order factor of Eq. (18b), the decoupled realization is obtained by a rearrangement of the first-order normalized lattice filter as shown in Fig. 8, where the coefficients d_0, d_1 are the solutions of the system:

$$\begin{bmatrix} 1 & \hat{a}_1 \\ \hat{a}_1 & 1 \end{bmatrix} \begin{bmatrix} d_0 \\ d_1 \end{bmatrix} = \begin{bmatrix} \hat{b}_0 \\ \hat{b}_1 \end{bmatrix} \quad (76)$$

Eq. (76) is equivalent to expanding the corresponding first-order transfer function in the form:

$$\frac{B(\hat{z})}{A(\hat{z})} = \frac{\hat{b}_0 + \hat{b}_1 \hat{z}^{-1}}{1 + \hat{a}_1 \hat{z}^{-1}} = d_0 + d_1 \frac{A^R(\hat{z})}{A(\hat{z})} \quad (77)$$

where $A^R(\hat{z})$ is the reverse of the polynomial $A(\hat{z})$. For the Butterworth first-order filter coefficients given by Eq. (22), we find:

$$\gamma_1 = \frac{\beta - 1}{\beta + 1}, \quad d_0 = \frac{g + g_0}{2}, \quad d_1 = \frac{g - g_0}{2} \quad (78)$$

Similarly, for the type-1 Chebyshev case, we have:

$$\gamma_1 = \frac{a\Omega_B - 1}{a\Omega_B + 1}, \quad d_0 = \frac{1}{2} \left(\frac{b}{a} + g_0 \right), \quad d_1 = \frac{1}{2} \left(\frac{b}{a} - g_0 \right) \quad (79)$$

Thus, the coefficients d_0, d_1 depend only on the gain, and the coefficients γ_1, τ_1 , only on the bandwidth. The second-order factors in Eq. (18b) also admit a decoupled realization, but at the expense of doubling the number of delays. Fig. 9 shows this realization, where the coefficients d_0, d_1, d_2 are the solutions of the system:

$$\begin{bmatrix} 1 & \hat{a}_2 & 1 \\ \hat{a}_1 & \hat{a}_1 & 2 \\ \hat{a}_2 & 1 & 1 \end{bmatrix} \begin{bmatrix} d_0 \\ d_1 \\ d_2 \tau_1 \tau_2 \end{bmatrix} = \begin{bmatrix} \hat{b}_0 \\ \hat{b}_1 \\ \hat{b}_2 \end{bmatrix} \quad (80)$$

This is equivalent to expanding the second-order transfer function (66) in the form:

$$\frac{B(\hat{z})}{A(\hat{z})} = d_0 + d_1 \frac{A^R(\hat{z})}{A(\hat{z})} + d_2 \frac{\tau_1 \tau_2 (1 + \hat{z}^{-1})^2}{A(\hat{z})} \quad (81)$$

For the i th second-order Butterworth factors of Eq. (22), we have:

$$d_0 = \frac{1}{2}g_0(g_0 + g), \quad d_1 = \frac{1}{2}g_0(g_0 - g), \quad d_2 = (g^2 - g_0^2) \sqrt{\frac{\beta(\beta^2 + 1)}{32s_i}} \quad (82)$$

with the reflection coefficients given by Eq. (70). For the type-1 Chebyshev case, we have:

$$y_1 = \frac{(a^2 + c_i^2)\Omega_B^2 - 1}{(a^2 + c_i^2)\Omega_B^2 + 1}, \quad y_2 = \frac{(a^2 + c_i^2)\Omega_B^2 - 2as_i\Omega_B + 1}{(a^2 + c_i^2)\Omega_B^2 + 2as_i\Omega_B + 1}$$

$$d_0 = \frac{1}{2}g_0 \left(g_0 + \frac{b}{a} \right), \quad d_1 = \frac{1}{2}g_0 \left(g_0 - \frac{b}{a} \right), \quad d_2 = (b^2 - g_0^2 a^2) \sqrt{\frac{((a^2 + c_i^2)\Omega_B^2 + 1)\Omega_B}{32s_i a (a^2 + c_i^2)}}$$

Replacing the unit delays \hat{z}^{-1} by Fig. 4, and splitting the multiplier d_2 into two factors, one depending on g and the other on Ω_B , we obtain a realization of the equalizer that allows the independent control of the gain, bandwidth, and center frequency. In the Chebyshev cases, one must choose $\alpha \ll 1$ for type-1 and $\alpha \gg 1$ for type-2 in Eq. (54), in order to achieve flat passbands and stopbands, respectively.

The main limitation of such decoupled realizations is the restrictive definition of the bandwidth level G_B . Thus, the transposed, normalized-lattice, and state-space realizations are more flexible.

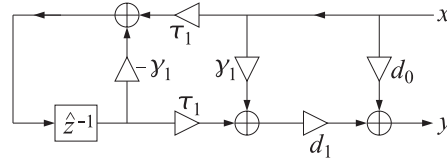


Fig. 8 Decoupled realization of the first-order factor of Eq. (18b).

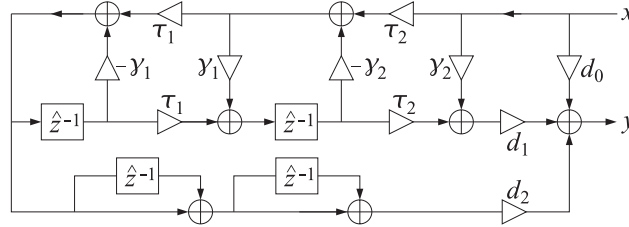


Fig. 9 Decoupled realization of the second-order factors of Eq. (18b).

9. Design Examples

Figures 10-13 show the magnitude response of the cascade of four equalizer filters: a lowpass shelf, a boost, a cut, and a highpass shelf, designed according to the four filter types with analog filter orders of $N = 4$ and $N = 5$. The center frequencies, bandwidths, and boost gains (relative to $G_0 = 0$ dB) were taken to be:

$$\begin{aligned} f_1 &= 0 \text{ kHz}, & \Delta f_1 &= 1 \text{ kHz}, & G_1 &= 9 \text{ dB} \\ f_2 &= 4 \text{ kHz}, & \Delta f_2 &= 2 \text{ kHz}, & G_2 &= 12 \text{ dB} \\ f_3 &= 9 \text{ kHz}, & \Delta f_3 &= 2 \text{ kHz}, & G_3 &= -6 \text{ dB} \\ f_4 &= 20 \text{ kHz}, & \Delta f_4 &= 4 \text{ kHz}, & G_4 &= 6 \text{ dB} \end{aligned} \quad (83)$$

where all gains must be converted from dB to absolute units before used in the design equations. The sampling rate was 40 kHz.

For the Butterworth case, shown in Fig. 10, the bandwidth gains were chosen to be 3 dB below (or above, for the cut case) the peak gains, that is:

$$G_{B1} = 6 \text{ dB}, \quad G_{B2} = 9 \text{ dB}, \quad G_{B3} = -3 \text{ dB}, \quad G_{B4} = 3 \text{ dB} \quad (84)$$

The bullet dots on the graphs show the center and bandedge frequencies computed by Eq. (8). The conventional biquad equalizers (first order for the shelves), designed with the same specifications, are also shown in Fig. 10, both individually (dotted lines) and as their overall cascaded response (dashed line). Because of the slow rolloffs of the individual sections, the biquad cascaded response no longer meets the required specifications.

For the type-1 Chebyshev cases, shown in Fig. 11, we have kept the same center frequencies, bandwidths, and peak gains, but in order to achieve flat passbands, we have chosen the bandwidth gains to be 0.01 dB below the peak gains, that is,

$$G_{B1} = 8.99 \text{ dB}, \quad G_{B2} = 11.99 \text{ dB}, \quad G_{B3} = -5.99 \text{ dB}, \quad G_{B4} = 5.99 \text{ dB} \quad (85)$$

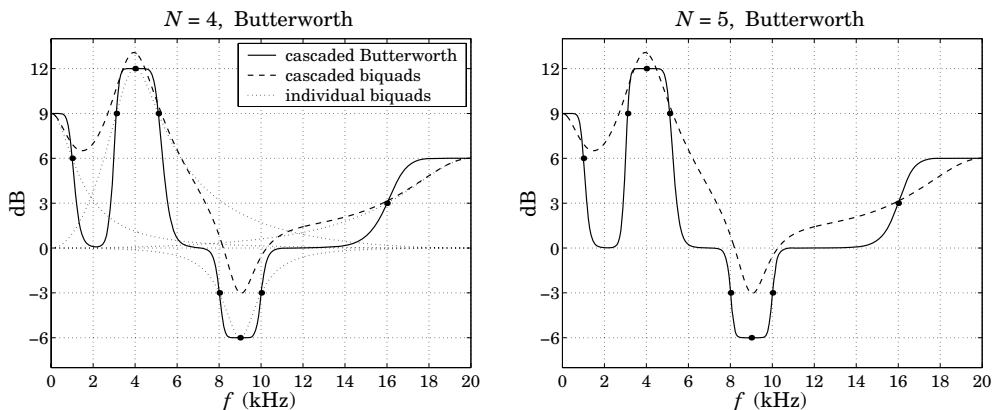


Fig. 10 Butterworth designs.

As a result, the passbands are very flat, but the only way to flatten the stopbands is to increase the rolloff rate by choosing larger values of the filter order N . For the type-2 Chebyshev cases, shown in Fig. 12, in order to achieve flat stopbands, we have chosen the bandwidth gains to be 0.01 dB above the 0-dB reference gain G_0 :

$$G_{B1} = 0.01 \text{ dB}, \quad G_{B2} = 0.01 \text{ dB}, \quad G_{B3} = -0.01 \text{ dB}, \quad G_{B4} = 0.01 \text{ dB} \quad (86)$$

The bandwidths near the reference gain line have the assumed values, but the equalizer peaks or cuts become narrower, with their width increasing with the filter order N . Fig. 13 shows the elliptic case, in which both the passband and stopband bandwidth gains were chosen to be 0.01 dB below the peaks and reference, that is, denoting the stopband gains by G_s :

$$\begin{aligned} G_{B1} &= 8.99 \text{ dB}, & G_{B2} &= 11.99 \text{ dB}, & G_{B3} &= -5.99 \text{ dB}, & G_{B4} &= 5.99 \text{ dB} \\ G_{s1} &= 0.01 \text{ dB}, & G_{s2} &= 0.01 \text{ dB}, & G_{s3} &= -0.01 \text{ dB}, & G_{s4} &= 0.01 \text{ dB} \end{aligned} \quad (87)$$

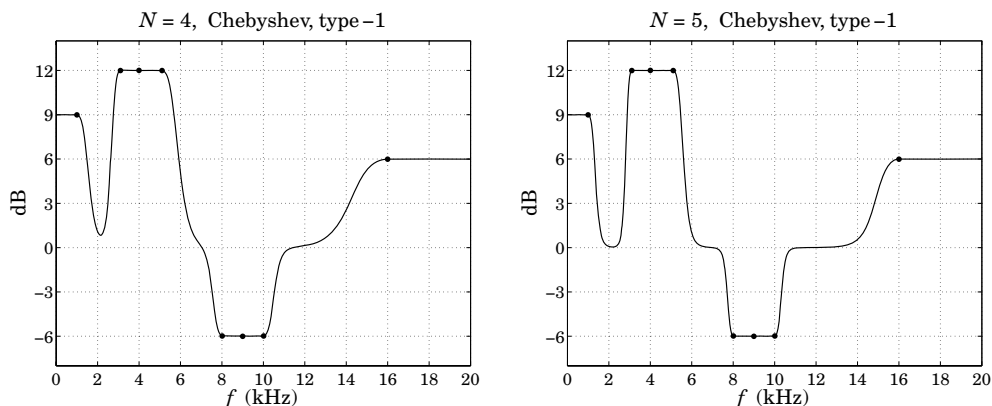


Fig. 11 Chebyshev type-1 designs.

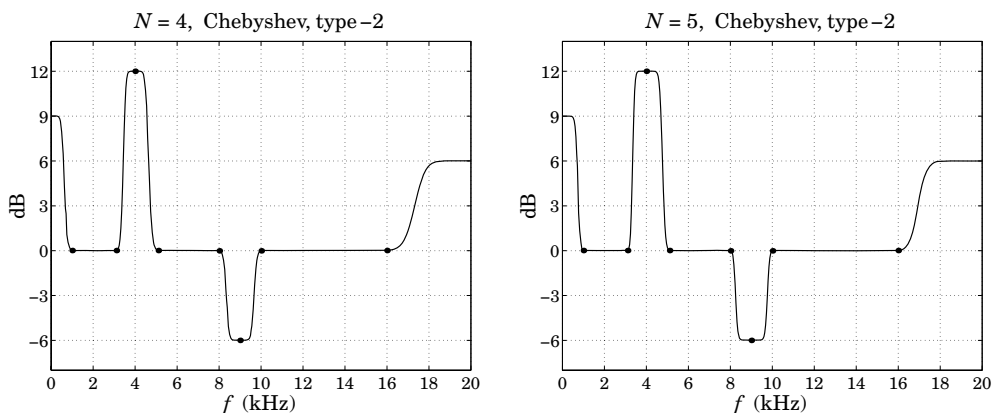


Fig. 12 Chebyshev type-2 designs.

The elliptic case combines the benefits of the type-1 and type-2 Chebyshev cases and achieves both flat passbands and stopbands.

To assess the accuracy of the elliptic function computations using a fixed number of Landen iterations (described in Appendix A.3), we have computed the percentage error in the overall cascaded frequency response and found that it is less than 0.1 percent if four iterations are used and less than 10^{-5} percent for five iterations, as compared to the case of maximum precision in which the tolerance was defined to be the machine epsilon. Thus, fixing the number of Landen iterations to five makes the implementation of the elliptic case only slightly more complicated than the Chebyshev cases.

Fig. 14 shows the same example, but redesigned so that the Chebyshev and elliptic cases have the same 3-dB widths as the Butterworth case. The bandwidths listed in Eq. (83) were taken to represent the 3-dB widths relative to the peak gains, that is, corresponding to the levels:

$$G_{b1} = 6 \text{ dB}, \quad G_{b2} = 9 \text{ dB}, \quad G_{b3} = -3 \text{ dB}, \quad G_{b4} = 3 \text{ dB} \quad (88)$$

The gains G_B and G_S were still defined by Eqs. (85)–(87). The 3-dB widths were remapped to the bandwidths at the G_B design levels using Eqs. (63)–(64). The analog filter order was $N = 4$.

We have compared also the performance of the canonical (direct-form-II), transposed, normalized lattice, and state-space realizations under some extreme filter settings with rapidly changing parameters. We used the same benchmark example discussed by Moorer [36], and applied Butterworth, Chebyshev, and elliptic equalizers of orders $N = 1$ -10 designed with the following gain specifications:

Butterworth:	$G = 18 \text{ dB}$,	$G_B = 15 \text{ dB}$
Chebyshev-1:	$G = 18 \text{ dB}$,	$G_B = 17.99 \text{ dB}$
Chebyshev-2:	$G = 18 \text{ dB}$,	$G_B = 0.01 \text{ dB}$
Elliptic:	$G = 18 \text{ dB}$,	$G_B = 17.99 \text{ dB}$, $G_S = 0.01 \text{ dB}$

For the first 1000 time samples, the center frequency and bandwidth (at level G_B) were fixed at 44.1 Hz and 22.05 Hz, respectively; for the next 2000 samples, the center frequency was

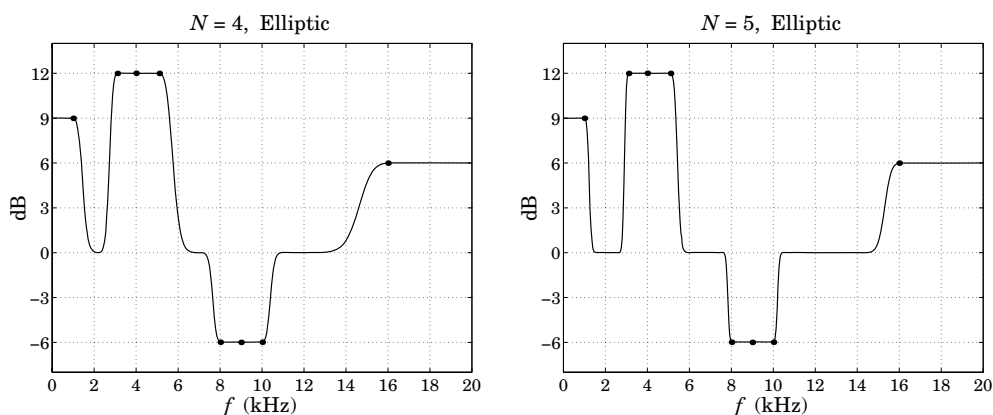


Fig. 13 Elliptic designs.

ramped up linearly to 441 Hz and the bandwidth to 220.5 Hz; and for the last 1000 samples they were kept fixed at 441 Hz and 220.5 Hz, respectively. The sampling rate was 44.1 kHz.

The input was a 4000-long vector of uniform random numbers in the range $[0, 1)$. The resulting outputs from the four realizations are shown in Fig. 15 for the elliptic design with $N = 5$. The graphs on the right column of the figure show the responses to a step-input of amplitude equal to 0.5, which corresponds to the mean of the random input.

The transposed realization was implemented as the cascade of the realizations of Fig. 5. The canonical realization was the transposed of Fig. 5. The normalized-lattice and the state-space realizations were implemented by cascading the realizations of Figs. 6 and 7, respectively.

We observe that the transposed, lattice, and state-space realizations yield comparable results. The outputs differ only during the middle period when the filter is time-varying and the realizations are not equivalent. Consistent with Moorer's observations [36], the normalized lattice output is visually indistinguishable from that of the state-space case—the two output signals differing by less than 0.2 percent. As expected, the canonical form suffers from larger oscillations during the middle period due to its unscaled internal states.

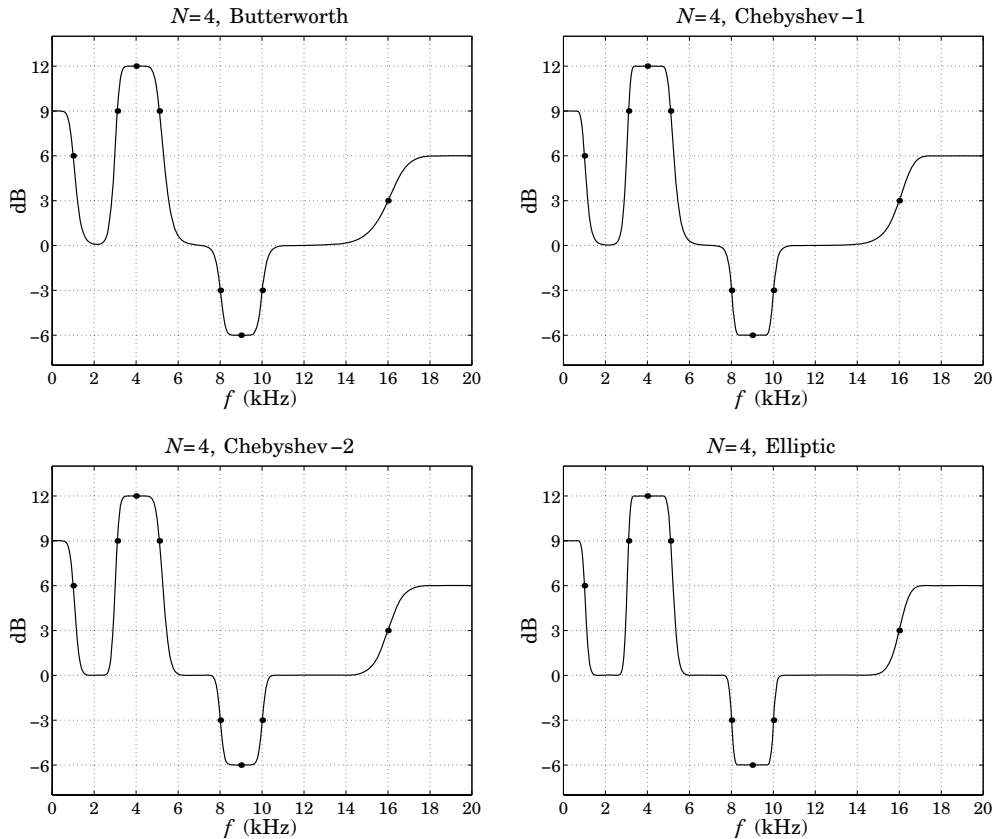


Fig. 14 Designs with common 3-dB widths.

The results from the Butterworth and Chebyshev designs and for orders $N = 1-10$ were comparable to those of Fig. 15. We have also varied the sampling rate up to 96 kHz and/or lowered all center frequencies with similar results. We looked specifically at the case when the initial center frequency was set to zero (a shelving filter) for the first 1000 samples. The canonical realization tended to deteriorate as the center frequencies got lower, resulting in large oscillations during the middle period; but the other realizations remained robust.

We also studied the performance of the transposed realizations of the fourth-order factors of Eq. (18c) and found that they were mostly well-behaved, but deteriorated at zero center frequencies, in fact, becoming unstable due to coefficient roundoff errors that pushed some of the poles outside the unit circle.

As a final example, we considered the behavior of the different realizations as the equalizer was being turned on and its gain and bandwidth were time-varying. The equalizer had a fixed

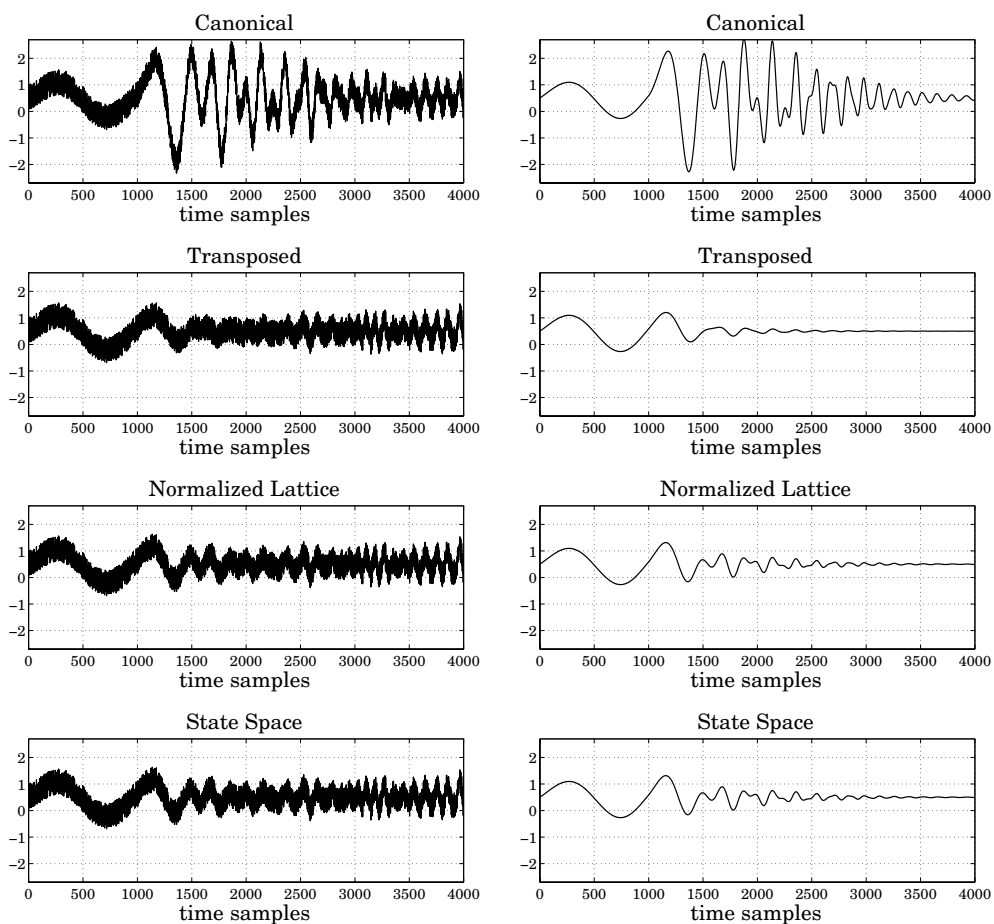


Fig. 15 Response of equalizer with time-varying center frequency and bandwidth.

center frequency of 400 Hz. The sampling rate was 44.1 kHz. The input was a 3000-sample long unit-amplitude sinusoid of frequency of 400 Hz. For the first 1000 samples, the equalizer was off; for the next 1000 samples, it was turned on with its bandwidth changing linearly from 20 Hz to 100 Hz and its peak gain changing from 0 dB to 18 dB; for the last 1000 samples, the bandwidth was fixed at 100 Hz and the gain at 18 dB.

Fig. 16 shows the outputs from the canonical, transposed, and normalized lattice realizations of an elliptic design with $N = 5$ and stopband level $G_s = 0.01$ dB. The bandwidth level G_B was taken to be 0.01 dB below the peak gain G (when these definitions could not be made because G was too small, we defined $G_B = \sqrt{G}$, and $G_s = \sqrt{G_B}$.) The state-space realization is not shown as it always produced virtually the same output as the lattice.

In the first row of graphs, the gain was switched on instantaneously to 18 dB ($G=8$ in absolute units); in the second row, it was turned on gradually in four steps that were linearly spaced in dB between 0 and 18 dB; and in the third row, the gain was increased continuously, varying linearly in dB. The gain curves have been superimposed on the graphs. Similar results were observed in the Butterworth and Chebyshev cases.

The gradual turning on of the equalizer [42–45] had the beneficial effect of eliminating undesirable overshoots (even two intermediate steps had the same positive effect.) Although the transposed realization was somewhat more sluggish in following the changing gain than the lattice, its lower computational cost and good numerical behavior make it a good choice for the implementation of high-order equalizers.

We also carried out the experiments of Figs. 15 and 16 using the decoupled realizations of Figs. 8 and 9 and found that they had virtually identical performance as the normalized lattice.

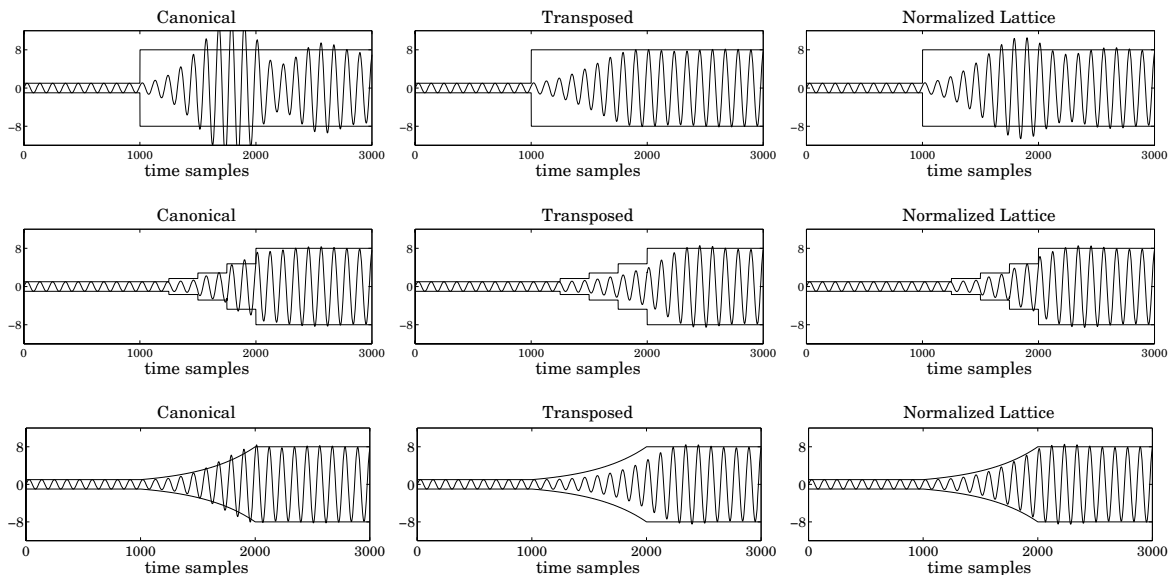


Fig. 16 Sinusoidal response of equalizer with time-varying gain.

10. Conclusion

We have presented a unified method of designing high-order digital parametric equalizers based on Butterworth, Chebyshev, and elliptic lowpass analog prototype filters. The high-order equalizers provide flatter passbands and/or stopbands and sharper bandedges. We considered the issues of choosing the filter order and bandwidth, and presented realizations based on frequency-shifted transposed, normalized-lattice, and state-space forms that have good numerical properties and are recommended for use under stringent and time-varying filter specifications. The design equations apply equally well to shelving filters, and to ordinary lowpass, highpass, bandpass, and bandstop filters.

Acknowledgements

I would like to thank Robert Bristow-Johnson, Martin Holters, Mark Kahrs, Florian Keiler, Dana Massie, James A. Moorer, and Udo Zölzer for their useful comments and suggestions.

References

- [1] K. Hirano, S. Nishimura, and S. Mitra, "Design of Digital Notch Filters," *IEEE Trans. Commun.*, COM-22, 964 (1974).
- [2] G. W. McNally, "Digital Audio: Recursive Digital Filtering for High Quality Audio Signals," BBC Research Dept. Report, BBC RD 1981/10, Dec. 1981. Available online from: www.bbc.co.uk/rd/pubs/reports/1981-10.pdf.
- [3] J. A. Moorer, "The Manifold Joys of Conformal Mapping: Applications to Digital Filtering in the Studio," *J. Audio Eng. Soc.*, 31, 826 (1983). Updated version available online from www.jamminpower.com.
- [4] S. A. White, "Design of a Digital Biquadratic Peaking or Notch Filter for Digital Audio Equalization," *J. Audio Eng. Soc.*, 34, 479 (1986).
- [5] P. A. Regalia and S. K. Mitra, "Tunable Digital Frequency Response Equalization Filters," *IEEE Trans. Acoust., Speech, Signal Process.*, ASSP-35, 118 (1987).
- [6] D. J. Shpak, "Analytical Design of Biquadratic Filter Sections for Parametric Filters," *J. Audio Eng. Soc.*, 40, 876 (1992).
- [7] D. C. Massie, "An Engineering Study of the Four-Multiply Normalized Ladder Filter," *J. Audio Eng. Soc.*, 41, 564 (1993).
- [8] F. Harris and E. Brooking, "A Versatile Parametric Filter Using Imbedded All-Pass Sub-Filter to Independently Adjust Bandwidth, Center Frequency, and Boost or Cut," Presented at the 95th Convention of the AES, New York, October 1993, *AES Preprint* 3757.

- [9] R. Bristow-Johnson, "The Equivalence of Various Methods of Computing Biquad Coefficients for Audio Parametric Equalizers," Presented at the 97th Convention of the AES, San Francisco, November 1994, *AES Preprint 3906*.
- [10] R. Bristow-Johnson, "Cookbook formulae for audio EQ biquad filter coefficients," available from: www.musicdsp.org/files/Audio-EQ-Cookbook.txt.
- [11] U. Zölzer and T. Boltze, "Parametric Digital Filter Structures," Presented at the 99th Convention of the AES, New York, October 1995, *AES Preprint 4099*.
- [12] U. Zölzer, *Digital Audio Signal Processing*, Wiley, Chichester, UK, 1997.
- [13] S. J. Orfanidis, *Introduction to Signal Processing*, Prentice Hall, Upper Saddle River, NJ, 1996.
- [14] S. J. Orfanidis, "Digital Parametric Equalizer Design With Prescribed Nyquist-Frequency Gain," *J. Aud. Eng. Soc.*, **45**, 444 (1997).
- [15] K. B. Christensen, "A Generalization of the Biquad Parametric Equalizer," Presented at the 115th Convention of the AES, New York, October 2003, *AES Preprint 5916*.
- [16] A. G. Constantinides, "Frequency Transformations for Digital Filters," *Elect. Lett.*, **3**, 487 (1967), and *ibid.*, **4**, 115 (1968).
- [17] A. G. Constantinides, "Spectral Transformations for Digital Filters," *Proc. IEE*, **117**, 1585 (1970).
- [18] F. Keiler and U. Zölzer, "Parametric Second- and Fourth-Order Shelving Filters for Audio Applications," *Proc. IEEE 6th Workshop on Multimedia Signal Processing*, Siena, Italy, Sept., 2004, p.231.
- [19] M. N. S. Swami and K. S. Thyagarajan, "Digital Bandpass and Bandstop Filters with Variable Center Frequency and Bandwidth," *Proc. IEEE*, **64**, 1632 (1976).
- [20] S. K. Mitra, Y. Neuvo, and H. Roivainen, "Design of Recursive Digital Filters with Variable Characteristics," *Int. J. Circ. Th. Appl.*, **18**, 107 (1990).
- [21] S. K. Mitra, K. Hirano, and S. Nishimura, "Design of Digital Bandpass/Bandstop Filters with Independent Tuning Characteristics," *Frequenz*, **44**, 117 (1990).
- [22] S. Darlington, "Synthesis of Reactance 4-Poles which Produce Prescribed Insertion Loss Characteristics," *J. Math. and Phys.*, **18**, 257 (1939).
- [23] R. W. Daniels, *Approximation Methods for Electronic Filter Design*, McGraw-Hill, New York, 1974.
- [24] H. J. Orchard, "Adjusting the Parameters of Elliptic Function Filters," *IEEE Trans. Circuits Syst., I*, **37**, 631 (1990).
- [25] H. J. Orchard and A. N. Willson, "Elliptic Functions for Filter Design," *IEEE Trans. Circuits Syst., I*, **44**, 273 (1997).

- [26] A. Antoniou, *Digital Filters*, 2nd ed., McGraw-Hill, New York, 1993.
- [27] M. D. Lutovac, D. V. Tasic, and B. L. Evans, *Filter Design for Signal Processing*, Prentice Hall, Upper Saddle River, NJ, 2001.
- [28] M. Vlcek and R. Unbehauen, "Degree, Ripple, and Transition Width of Elliptic Filters," *IEEE Trans. Circ. Syst.*, **CAS-36**, 469 (1989).
- [29] C. G. J. Jacobi, "Fundamenta Nova Theoriae Functionum Ellipticarum," reprinted in *C. G. J. Jacobi's Gesammelte Werke*, vol.1, C. W. Borchardt, ed., Verlag von G. Reimer, Berlin, 1881.
- [30] D. F. Lawden, *Elliptic Functions and Applications*, Springer-Verlag, New York, 1989.
- [31] P. F. Byrd and M. D. Friedman, *Handbook of Elliptic Integrals for Engineers and Scientists*, Springer-Verlag, New York, 1971.
- [32] R. Bristow-Johnson, Private Communication, June 2005.
- [33] R. A. Losada and V. Pellissier, "Designing IIR Filters with a Given 3-dB Point," *IEEE Signal Process. Mag.*, **22**, no.4, 95, July 2005.
- [34] A. H. Gray and J. D. Markel, "A Normalized Digital Filter Structure," *IEEE Trans. Acoust., Speech, Signal Process.*, **ASSP-23**, 268 (1975).
- [35] A. H. Gray and J. D. Markel, "Roundoff Noise Characteristics of a Class of Orthogonal Polynomial Structures," *IEEE Trans. Acoust., Speech, Signal Process.*, **ASSP-23**, 473 (1975).
- [36] J. A. Moorer, "48-Bit Integer Processing Beats 32-Bit Floating Point for Professional Audio Applications," Presented at the 107th Convention of the AES, New York, September 1999, *AES Preprint 5038*.
- [37] C. T. Mullis and R. A. Roberts, "Synthesis of Minimum Roundoff Noise Fixed-Point Digital Filters," *IEEE Trans. Circuits Syst.*, **CAS-23**, 551 (1976).
- [38] S. Y. Hwang, "Minimum Uncorrelated Unit Noise in State-Space Digital Filtering," *IEEE Trans. Acoust., Speech, Signal Process.*, **ASSP-25**, 273 (1977).
- [39] C. T. Mullis and R. A. Roberts, *Digital Signal Processing*, Addison-Wesley, Boston, 1987.
- [40] C. W. Barnes, "On the Design of Optimal State-Space Realizations of Second-Order Digital Filters," *IEEE Trans. Circuits Syst.*, **CAS-31**, 602 (1984).
- [41] B. W. Bomar, "New Second-Order State-Space Structures for Realizing Low Roundoff Noise Digital Filters," *IEEE Trans. Acoust., Speech, Signal Process.*, **ASSP-33**, 106 (1985).
- [42] J. N. Mourjopoulos, E. D. Kyriakis-Bitzaros, and C. E. Goutis, "Theory and Real-Time Implementation of Time-Varying Digital Audio Filters," *J. Aud. Eng. Soc.*, **38**, 523 (1990).
- [43] U. Zölzer, B. Redmer, and J. Bucholz, "Strategies for Switching Digital Audio Filters," Presented at the 95th Convention of the AES, New York, October 1993, *AES Preprint 3714*.

- [44] Y. Ding and D. Rossum, "Filter Morphing of Parametric Equalizers and Shelving Filters for Audio Signal Processing," *J. Aud. Eng. Soc.*, **43**, 821 (1995).
- [45] J. Laroche, "Using Resonant Filters for the Synthesis of Time-Varying Sinusoids," Presented at the 105th Convention of the AES, San Francisco, September 1998, *AES Preprint 4782*.
- [46] Available from from the author's web page: www.ece.rutgers.edu/~orfanidi/hpeq, and from this Journal's supplementary materials page: www.aes.org/journal/suppmat.

Appendix

A.1 Bilinear Transformations

The algebraic relationships among the coefficients of Eq. (18) are given as follows. For the s to \hat{z}^{-1} transformation, the first- and second-order section coefficients are:

$$\begin{aligned}
 D_0 &= A_{00} + A_{01} & D_i &= A_{i0} + A_{i1} + A_{i2} \\
 \hat{b}_{00} &= (B_{00} + B_{01})/D_0 & \hat{b}_{i0} &= (B_{i0} + B_{i1} + B_{i2})/D_i \\
 \hat{b}_{01} &= (B_{00} - B_{01})/D_0 & \hat{b}_{i1} &= 2(B_{i0} - B_{i2})/D_i \\
 \hat{a}_{01} &= (A_{00} - A_{01})/D_0 & \hat{b}_{i2} &= (B_{i0} - B_{i1} + B_{i2})/D_i \\
 & & \hat{a}_{i1} &= 2(A_{i0} - A_{i2})/D_i \\
 & & \hat{a}_{i2} &= (A_{i0} - A_{i1} + A_{i2})/D_i
 \end{aligned} \tag{89}$$

For the \hat{z}^{-1} to z^{-1} transformation, we obtain the second- and fourth-order coefficients:

$$\begin{aligned}
 b_{00} &= \hat{b}_{00} & b_{i0} &= \hat{b}_{i0} \\
 b_{01} &= c_0(\hat{b}_{01} - \hat{b}_{00}) & b_{i1} &= c_0(\hat{b}_{i1} - 2\hat{b}_{i0}) \\
 b_{02} &= -\hat{b}_{01} & b_{i2} &= (\hat{b}_{i0} - \hat{b}_{i1} + \hat{b}_{i2})c_0^2 - \hat{b}_{i1} \\
 a_{01} &= c_0(\hat{a}_{01} - 1) & b_{i3} &= c_0(\hat{b}_{i1} - 2\hat{b}_{i2}) \\
 a_{02} &= -\hat{a}_{01} & b_{i4} &= \hat{b}_{i2} \\
 & & a_{i1} &= c_0(\hat{a}_{i1} - 2) \\
 & & a_{i2} &= (1 - \hat{a}_{i1} + \hat{a}_{i2})c_0^2 - \hat{a}_{i1} \\
 & & a_{i3} &= c_0(\hat{a}_{i1} - 2\hat{a}_{i2}) \\
 & & a_{i4} &= \hat{a}_{i2}
 \end{aligned} \tag{90}$$

A.2 Poles and Zeros

The zeros and poles of the analog shelving filter $H_a(s)$ are constructed by by finding the roots of the numerator and denominator of Eq. (10), that is, solving:

$$G^2 + G_0^2 \varepsilon^2 F_N^2(w) = 0, \quad 1 + \varepsilon^2 F_N^2(w) = 0 \tag{91}$$

or, equivalently,

$$F_N(w) = \pm j \frac{G}{G_0 \varepsilon}, \quad F_N(w) = \pm j \frac{1}{\varepsilon} \quad (92)$$

For the *Butterworth case*, we have $F_N(w) = w^N$, which leads to the following left-hand s -plane zeros and poles:

$$z_0 = -\frac{g\beta}{g_0}, \quad z_i = \frac{g\beta}{g_0}(-s_i + jc_i), \quad p_0 = -\beta, \quad p_i = \beta(-s_i + jc_i) \quad (93)$$

for $i = 1, 2, \dots, L$, where we introduced the parameters:

$$g = G^{1/N}, \quad g_0 = G_0^{1/N}, \quad \beta = \varepsilon^{-1/N} \Omega_B = \varepsilon^{-1/N} \tan\left(\frac{\Delta\omega}{2}\right) \quad (94)$$

$$s_i = \sin \phi_i, \quad c_i = \cos \phi_i, \quad \phi_i = \frac{(2i-1)\pi}{2N}, \quad i = 1, 2, \dots, L \quad (95)$$

Eq. (19) was obtained by multiplying out the first-order zero and pole factors and distributing the gain $H_0 = G = g^N$ over the N first-order sections of Eq. (13).

For the *type-1 Chebyshev case*, we have $F_N(w) = C_N(w)$ and the left-hand s -plane zeros and poles are found to be:

$$\begin{aligned} z_0 &= -\Omega_B \sinh u, & z_i &= j\Omega_B \cos(\phi_i - ju) = \Omega_B(-s_i \sinh u + jc_i \cosh u) \\ p_0 &= -\Omega_B \sinh v, & p_i &= j\Omega_B \cos(\phi_i - jv) = \Omega_B(-s_i \sinh v + jc_i \cosh v) \end{aligned} \quad (96)$$

where $i = 1, 2, \dots, L$, and s_i, c_i, ϕ_i are the same as in Eq. (95). The quantities u, v are given by:

$$e^u = g_0^{-1} \beta, \quad \beta = (G\varepsilon^{-1} + G_B \sqrt{1 + \varepsilon^{-2}})^{1/N}, \quad e^v = \alpha = (\varepsilon^{-1} + \sqrt{1 + \varepsilon^{-2}})^{1/N} \quad (97)$$

where $g_0 = G_0^{1/N}$. The transfer function (24) was obtained by inserting (96) into Eq. (15) and distributing the gain $H_\infty = G_0 = g_0^N$ over the N first-order sections.

For the *type-2 Chebyshev case*, we have $F_N(w) = 1/C_N(1/w)$, which leads to zeros and poles that are essentially the inverses of those of Eq. (96). For $i = 1, 2, \dots, L$, we have:

$$\begin{aligned} z_0^{-1} &= -\Omega_B^{-1} \sinh u, & z_i^{-1} &= j\Omega_B^{-1} \cos(\phi_i - ju) = \Omega_B^{-1}(-s_i \sinh u + jc_i \cosh u) \\ p_0^{-1} &= -\Omega_B^{-1} \sinh v, & p_i^{-1} &= j\Omega_B^{-1} \cos(\phi_i - jv) = \Omega_B^{-1}(-s_i \sinh v + jc_i \cosh v) \end{aligned} \quad (98)$$

where s_i, c_i, ϕ_i are the same as in Eq. (95), and the quantities u, v are defined by:

$$e^u = g^{-1} \beta, \quad \beta = (G_0 \varepsilon + G_B \sqrt{1 + \varepsilon^2})^{1/N}, \quad e^v = \alpha = (\varepsilon + \sqrt{1 + \varepsilon^2})^{1/N} \quad (99)$$

where $g = G^{1/N}$. Inserting these into Eq. (13) and distributing the gain $H_0 = G = g^N$ over the N first-order sections, we obtain the analog transfer function (30).

We note that in both Chebyshev cases, the shelving zeros z_i (or their inverses in type-2) as well as the poles p_i , lie on an ellipse on the s -plane, while in the Butterworth case they lie on a circle.

In the *elliptic case*, we have $F_N(w) = \text{cd}(uK_1, k_1)$ with $w = \text{cd}(uK, k)$. Assuming initially that $G \neq 0$ and $G_0 \neq 0$, the resulting left-hand s -plane zeros and poles of $H_a(s)$ in Eq. (13) are given as follows, for $i = 1, 2, \dots, L$:

$$z_i = j\Omega_B \text{cd}((u_i - ju_0)K, k), \quad p_i = j\Omega_B \text{cd}((u_i - jv_0)K, k) \quad (100)$$

where the $u_i = (2i - 1)/N$ are the same as in Eq. (37), and u_0, v_0 are real-valued and are the solutions of the equations:

$$\text{sn}(ju_0NK_1, k_1) = j\frac{G}{G_0\varepsilon}, \quad \text{sn}(jv_0NK_1, k_1) = j\frac{1}{\varepsilon} \quad (101)$$

If N is odd, there is an additional real-valued zero and pole obtained from Eq. (100) by setting $u_i = 1$ (which corresponds to the index $i = L + 1$):

$$\begin{aligned} z_0 &= j\Omega_B \text{cd}((1 - ju_0)K, k) = j\Omega_B \text{sn}(ju_0K, k) \\ p_0 &= j\Omega_B \text{cd}((1 - jv_0)K, k) = j\Omega_B \text{sn}(jv_0K, k) \end{aligned} \quad (102)$$

where we used the identity [31]: $\text{cd}(K - x, k) = \text{sn}(x, k)$. The evaluation of the elliptic functions cd and sn and their inverses can be carried out efficiently by means of the Landen transformation described in Appendix A.3.

Working with the normalized frequency $w_i = z_i/j\Omega_B = \text{cd}((u_i - ju_0)K, k)$, we verify the root condition (92):

$$\begin{aligned} F_N(w_i) &= \text{cd}((u_i - ju_0)NK_1, k_1) = \text{cd}((2i - 1)K_1 - ju_0NK_1, k_1) \\ &= (-1)^i \text{sn}(ju_0NK_1, k_1) = \pm j\frac{G}{G_0\varepsilon} \end{aligned}$$

where we used the property [31]: $\text{cd}((2i - 1)K_1 + x, k_1) = (-1)^i \text{sn}(x, k_1)$, for integer i . Similarly, for odd N we have $\text{cd}((1 - ju_0)NK_1, k_1) = \text{sn}(ju_0NK_1, k_1) = jG/(G_0\varepsilon)$.

The two special cases $G_0 = 0$ and $G = 0$ must be treated separately because they lead to the values $z_0 = \infty$ and $z_0 = 0$ in Eq. (102). When $G_0 = 0$, Eq. (10) implies that the zeros of $H_a(s)$ coincide with the poles of $F_N(w)$, which were defined in Eq. (37). Thus, the conjugate zeros are:

$$z_i = j\Omega_B (k\zeta_i)^{-1}, \quad \zeta_i = \text{cd}(u_iK, k) \quad (103)$$

The same conclusion can also be drawn by noting that when $G_0 = 0$ the solution of Eq. (101) is $ju_0NK_1 = jK'_1$, that is, it corresponds to a pole of the $\text{sn}(x, k_1)$ function. But because of the degree equation, we also have $ju_0K = jK'$, which is a pole of the $\text{sn}(x, k)$ function. Therefore, $z_0 = \infty$ and the zero factor $(1 - s/z_0)$ of $H_a(s)$ may be replaced by unity. Using the identity $\text{cd}(x - jK', k) = 1/(k \text{cd}(x, k))$, the expression (100) for z_i reduces to (103) for this value of u_0 .

When $G = 0$, the zeros of $H_a(s)$ coincide with the zeros of $F_N(w)$ given by Eq. (37), but there is an extra zero at $z_0 = 0$ for the odd- N case. The factor $(1 - s/z_0)$ of Eq. (13) must be handled as a limiting case as $G \rightarrow 0$. Using the Taylor series expansion $\text{sn}(x, k) \simeq x$, which is valid for small x , it follows that when G is small, the solution of Eq. (101) for u_0 , and the zero z_0 of Eq. (102), are given approximately by:

$$ju_0NK_1 \simeq j\frac{G}{G_0\varepsilon} \Rightarrow u_0 \simeq \frac{G}{G_0\varepsilon NK_1}, \quad z_0 = j\Omega_B \text{sn}(ju_0K, k) \simeq -\Omega_B u_0 K = -\frac{\Omega_B GK}{G_0\varepsilon NK_1}$$

Because in the odd- N case the overall gain in Eq. (13) is $H_0 = G$, it follows that the first-order factor $H_0(1 - s/z_0)$ of the transfer function will have a finite limit as $G \rightarrow 0$:

$$H_0(1 - s/z_0) \simeq G + G \frac{s G_0 \varepsilon N K_1}{\Omega_B G K} \rightarrow \frac{s}{\Omega_B} G_0 \varepsilon \frac{N K_1}{K}$$

Thus, in the odd- N case, the first-order numerator factor of Eq. (13) takes the following forms:

$$H_0(1 - s/z_0) = \begin{cases} G(1 - s/z_0), & \text{if } G_0 \neq 0, G \neq 0 \\ G, & \text{if } G_0 = 0, G \neq 0 \\ (s/\Omega_B)(G_0 \varepsilon)(N K_1/K), & \text{if } G_0 \neq 0, G = 0 \end{cases} \quad (104)$$

For the even- N case, we have $H_0 = G_B$, per Eq. (14). Similarly, the conjugate zeros z_i , $i = 1, 2, \dots, L$, are given as follows, for both even and odd N :

$$z_i = \begin{cases} j\Omega_B \operatorname{cd}((u_i - ju_0)K, k), & \text{if } G_0 \neq 0, G \neq 0 \\ j\Omega_B (k\zeta_i)^{-1}, & \text{if } G_0 = 0, G \neq 0 \\ j\Omega_B \zeta_i, & \text{if } G_0 \neq 0, G = 0 \end{cases} \quad (105)$$

The case $G_0 = 0, G \neq 0$ corresponds, of course, to the conventional designs of analog lowpass elliptic filters [22-27].

A.3 Elliptic Function Computations

The key tool for the required elliptic function calculations is the Landen transformation [25,31], which starts with a given elliptic modulus k and generates a sequence of decreasing moduli k_n via the following recursion, initialized at $k_0 = k$:

$$k_n = \left(\frac{k_{n-1}}{1 + k'_{n-1}} \right)^2, \quad n = 1, 2, \dots, M \quad (106)$$

where $k'_{n-1} = (1 - k_{n-1}^2)^{1/2}$. The moduli k_n decrease rapidly to zero. The recursion is stopped at $n = M$ when k_M has become smaller than a specified tolerance level, for example, smaller than the machine epsilon. For all practical values of k , such as those in the range $0 \leq k \leq 0.999$, the recursion may be stopped at $M = 5$, with all subsequent k_n being smaller than 10^{-15} , while for $k \leq 0.99$, the subsequent k_n remain smaller than 10^{-20} .

The Landen recursions (106) imply the following recursions [31] for the complete elliptic integrals K_n, K'_n corresponding to the moduli k_n, k'_n :

$$\begin{aligned} K_{n-1} &= (1 + k_n)K_n \\ K'_{n-1} &= (1 + k_n)K'_n/2 \end{aligned} \quad \Rightarrow \quad 2 \frac{K'_{n-1}}{K_{n-1}} = \frac{K'_n}{K_n} \quad (107)$$

Eq. (107) corresponds to the degree equation with $N = 2$. In fact, Eq. (106) is the same as Eq. (41) with $L = 1$ and $u_1 = 1/2$, that is, $k_n = k_{n-1}^2 \operatorname{sn}^4(u_1 K_{n-1}, k_{n-1})$, where (106) follows from the property $\operatorname{sn}(K/2, k) = 1/\sqrt{1 + k'}$. The recursion (107) can be repeated to compute the

elliptic integral $K = K(k)$, that is, $K = K_0 = (1 + k_1)K_1 = (1 + k_1)(1 + k_2)K_2$, and so on, yielding:

$$K = (1 + k_1)(1 + k_2) \cdots (1 + k_M)K_M, \quad K_M = \frac{\pi}{2} \quad (108)$$

Because k_M is almost zero, its elliptic integral will be essentially equal to $K_M = \pi/2$. The elliptic integral K' can be computed in the same way by applying the Landen recursion to k' .

The Landen transformations allow the efficient evaluation of the elliptic functions cd and sn via the following backward recursion, known also as the Gauss transformation [31], and written in the notation of Ref. [25]:

$$\frac{1}{\text{cd}(uK_{n-1}, k_{n-1})} = \frac{1}{1 + k_n} \left[\frac{1}{\text{cd}(uK_n, k_n)} + k_n \text{cd}(uK_n, k_n) \right] \quad (109)$$

for $n = M, M-1, \dots, 1$. The recursion is initialized at $n = M$ where k_M is so small that the cd function is indistinguishable from a cosine, that is, $\text{cd}(uK_M, k_M) \simeq \cos(u\pi/2)$. Thus, the computation of $w = \text{cd}(uK, k)$, at any complex value of u , proceeds by calculating the quantities $w_n = \text{cd}(uK_n, k_n)$, initialized at $w_M = \cos(u\pi/2)$, and ending with $w_0 = w = \text{cd}(uK, k)$:

$$w_{n-1}^{-1} = \frac{1}{1 + k_n} [w_n^{-1} + k_n w_n], \quad n = M, M-1, \dots, 1 \quad (110)$$

The function $w = \text{sn}(uK, k)$ can be evaluated by the same recursion, initialized at $w_M = \sin(u\pi/2)$. The recursion (110) can also be used to calculate the inverse cd and sn functions by inverting it to proceed forward from $n = 0$ to $n = M$:

$$w_n^{-1} = \frac{1 + k_n}{2} \left[w_{n-1}^{-1} + \sqrt{w_{n-1}^{-2} - k_{n-1}^2} \right], \quad n = 1, 2, \dots, M \quad (111)$$

Starting with a given complex value $w = \text{cd}(uK, k)$, and setting $w_0 = w$, the recursion will end at $w_M = \cos(u\pi/2)$, which may be inverted to yield $u = (2/\pi) \text{acos}(w_M)$. Because u is not unique, it may be reduced to lie within the period strip, $0 \leq \text{Im}(u) < 2K'/K$. The inverse of $w = \text{sn}(uK, k)$ is obtained from the same recursion, but with $u = (2/\pi) \text{asin}(w_M)$.

The evaluation of the cd elliptic function at a complex argument can also be carried out via the addition theorem [31]:

$$\text{cd}(u + jv, k) = \frac{\text{cn}(u, k) \text{cn}(v, k') - j \text{sn}(u, k) \text{dn}(u, k) \text{sn}(v, k') \text{dn}(v, k')}{\text{dn}(u, k) \text{cn}(v, k') \text{dn}(v, k') - jk^2 \text{sn}(u, k) \text{cn}(u, k) \text{sn}(v, k')} \quad (112)$$

Finally, we note the following identity, valid for even N with the u_i defined as in Eq. (37):

$$\prod_{i=1}^L \text{cd}(u_i K, k) = \prod_{i=1}^L \text{sn}(u_i K, k) \quad (113)$$

where $N = 2L$. It may be used to derive the values of the function $F_N(w)$ at $w = 0$ and $w = \infty$, that is, $F_{2L}(0) = (-1)^L$ and $F_{2L}(\infty) = (-1)^L/k_1$. From these, one may derive Eqs. (14) and (16).

The MATLAB toolbox described in Appendix A.6 contains functions for the implementation of all of the above operations.

A.4 State-Space Realizations

Given the numerator and denominator coefficients of a second-order transfer function of the form of Eq. (66) with complex-conjugate poles, the optimum minimum roundoff-error state-space realization is constructed by the following steps [40]:

$$\begin{aligned}
\sigma &= -\frac{\hat{a}_1}{2}, \quad \omega = \sqrt{\hat{a}_2 - \frac{\hat{a}_1^2}{4}}, \quad p = \sigma + j\omega \\
q_1 &= \hat{b}_1 - \hat{b}_0\hat{a}_1, \quad q_2 = \hat{b}_2 - \hat{b}_0\hat{a}_2 \\
\alpha_r &= \frac{q_1}{2}, \quad \alpha_i = -\frac{q_1\sigma + q_2}{2\omega}, \quad \alpha = \alpha_r + j\alpha_i \\
P &= \frac{|\alpha|}{1 - |p|^2}, \quad Q = \text{Im} \left[\frac{\alpha}{1 - p^2} \right], \quad k = \sqrt{\frac{P+Q}{P-Q}} \\
B_1 &= \sqrt{\frac{|\alpha| - \alpha_i}{P-Q}}, \quad B_2 = -\text{sign}(\alpha_r) \sqrt{\frac{|\alpha| + \alpha_i}{P+Q}} \\
C_1 &= \frac{\alpha_r}{B_1}, \quad C_2 = \frac{\alpha_r}{B_2}
\end{aligned} \tag{114}$$

which define the $ABCD$ state-space parameters:

$$A = \begin{bmatrix} \sigma & \omega k \\ -\omega/k & \sigma \end{bmatrix}, \quad B = \begin{bmatrix} B_1 \\ B_2 \end{bmatrix}, \quad C = [C_1, C_2], \quad D = \hat{b}_0 \tag{115}$$

In the special case when $\alpha_r = 0$ and $\alpha_i > 0$, we have:

$$B_1 = 0, \quad B_2 = -\sqrt{\frac{2|\alpha|}{P+Q}}, \quad C_1 = \sqrt{2|\alpha|(P-Q)}, \quad C_2 = 0 \tag{116}$$

and in the case, $\alpha_r = 0$ and $\alpha_i < 0$:

$$B_1 = \sqrt{\frac{2|\alpha|}{P-Q}}, \quad B_2 = 0, \quad C_1 = 0, \quad C_2 = -\sqrt{2|\alpha|(P+Q)} \tag{117}$$

The condition that the poles be conjugate pairs is equivalent to the reality of the quantity ω . This condition is guaranteed by the bilinear transformation construction of the factors of Eq. (18b). For the first-order factor of (18b), we may define $B_1 = (1 - \hat{a}_1^2)^{1/2}$ and:

$$A = \begin{bmatrix} -\hat{a}_1 & 0 \\ 0 & 0 \end{bmatrix}, \quad B = \begin{bmatrix} B_1 \\ 0 \end{bmatrix}, \quad C = [q_1/B_1, 0], \quad D = \hat{b}_0 \tag{118}$$

A.5 Analog Equalizer Design

The design of analog equalizers requires only some minor changes. The lowpass analog shelving filter of Eq. (18a) is designed exactly as before, but with the design parameter $\Omega_B = \Delta\omega$, where

$\Delta\omega = 2\pi\Delta f$ is the desired bandwidth in radians per second. The shelving filter is transformed into an analog bandpass equalizer by the s -domain frequency transformation:

$$s \rightarrow s + \frac{\omega_0^2}{s} \quad (119)$$

where $\omega_0 = 2\pi f_0$ is the desired center frequency in rads/second. Eq. (119) turns the first- and second-order sections of Eq. (18a) into second- and fourth-order sections in s .

The bandedge frequencies are calculated by $\omega_{2,1} = \pm\Delta\omega/2 + (\omega_0^2 + \Delta\omega^2/4)^{1/2}$. They satisfy $\omega_0^2 = \omega_1\omega_2$ and $\Delta\omega = \omega_2 - \omega_1$. In octaves, we have $\omega_1 = 2^{-B/2}\omega_0$, $\omega_2 = 2^{B/2}\omega_0$, and $\Delta\omega = 2\omega_0 \sinh(B \ln(2)/2)$.

For a lowpass shelving filter, one must use $\Omega_B = \omega_c$, where $\omega_c = 2\pi f_c$ is the cutoff frequency defined at level G_B . For the highpass case, one must start the lowpass design with $\Omega_B = 1/\omega_c$, and apply the highpass transformation $s \rightarrow 1/s$.

A.6 MATLAB Functions

We developed a set of MATLAB functions for implementing the designs and filtering operations discussed in this paper. These functions, as well as the scripts used to generate all of the examples of Sect. 9, may be downloaded from the author's web page [46]. The set does not require any additional toolboxes and contains the following functions:

<code>hpeq</code>	high-order parametric equalizer design, Sections 2-5
<code>hpeqex0,1,2</code>	examples illustrating the usage of <code>hpeq</code>
<code>blt</code>	LP-to-BP bilinear transformation, Eqs. (17), (89)-(90)
<code>bandedge</code>	bandedge frequencies, Eqs. (8) and (45)
<code>hpeqord</code>	determine filter order from specifications, Eqs. (46)-(49)
<code>octbw</code>	octave to linear bandwidth calculation, Eqs. (58)-(61)
<code>hpeqbw</code>	bandwidth remapping, Eqs. (63)-(64)
<code>fresp</code>	frequency response of cascaded sections, Eqs. (18b) and (18c)
<code>dir2latt</code>	direct-form to normalized lattice coefficients, Eqs. (67)-(68)
<code>dir2state</code>	direct-form to state-space parameters, Eqs. (114)-(118)
<code>dir2decoup</code>	direct-form to decoupled realization, Eqs. (76)-(82)
<code>transpfilt</code>	filtering in cascaded transposed form, Fig. 5
<code>nlattfilt</code>	filtering in cascaded normalized lattice form, Fig. 6
<code>df2filt</code>	filtering in direct-form-II realized by the transposed of Fig. 5
<code>statefilt</code>	filtering in cascaded state-space form, Fig. 7
<code>decoupfilt</code>	filtering in cascaded decoupled form, Figs. 8-9
<code>stpeq</code>	state-space biquad parametric equalizer, Eq. (73)
<code>landen</code>	Landen transformation, Eq. (106)
<code>cde,acde</code>	cd elliptic function and its inverse, Eqs. (110)-(111)
<code>sne,asne</code>	sn elliptic function and its inverse, Eqs. (110)-(111)
<code>cne,dne</code>	cn and dn elliptic functions (for real arguments)
<code>ellipk</code>	complete elliptic integral $K(k)$, Eq. (108)
<code>ellipdeg</code>	exact solution of degree equation (k from N, k_1), Eq. (42)
<code>ellipdeg1</code>	exact solution of degree equation (k_1 from N, k), Eq. (41)
<code>ellipdeg2</code>	solution of degree equation using nomes, Eq. (44)
<code>elliprf</code>	elliptic rational function, Eq. (36)

In addition, there are some scripts for testing the filtering algorithms of Sect. 8 and the convergence of the iteration (61). Moreover, the functions `hpeq_a`, `hpeqord_a`, `bandedge_a`, `hpeqbw_a`, `hpeqex1_a`, and `fresp_a` allow the design of *analog* parametric equalizers and shelving filters.